Adenosine Deaminating/ Hydrolyzing Enzymes from Alaska pea seeds (*Pisum sativum*)

by

Lendsey Breanna Thicklin

A Thesis Submitted to the
Faculty of the College of Graduate Studies
in Partial Fulfillment of
the Requirements for the Degree of
Master of Science
in Chemistry

Middle Tennessee State University
August 2017

Thesis Committee:

Dr. Paul C. Kline, Chair

Dr. Donald A. Burden

Dr. Justin M. Miller

I dedicate this thesis research to my ancestors, parents, siblings, mentors, line sisters, and college friends. You all fuel my drive to reach for all of my dreams; no matter how big or small.

"Thicklin's make a difference, we don't give up" - Dad

ACKNOWLEDGEMENTS

ABSTRACT

Nucleoside deaminases and nucleoside hydrolases are essential within the purine salvage pathway to recycle purine bases to promote cellular functions such as DNA synthesis, cytokinin metabolism, and more. Plants such as the Alaska pea (*Pisum sativum*) rely heavily on these enzymes, yet the enzymatic and structural characterizations of these proteins are limited. A 67 kilodalton (kDa) protein was isolated from germinated Alaska pea seeds with a 103 fold purification and 2.8 % recovery. The analysis of the enzymatic activity of this protein revealed adenosine is metabolized to inosine, adenine, and hypoxanthine suggesting a bifunctional enzyme combining nucleosidase and deaminase activities. This dimeric protein had an inosine Michaelis constant of 268 μM ± 78 μM. The optimum pH for enzymatic activity was determined to be pH 6. Research involving plant based nucleoside deaminases and nucleoside hydrolases can provide an origin of reference in the development of compounds that can be used as herbicides.

TABLE OF CONTENTS

LIST OF FIGURES

LIST OF TABLES

CHAPTER I

INTRODUCTION

There are billions of organisms that have been classified by scientists; each organism differers by size, degree of genomic complexity, and more. However, these drastic differences between organisms at the macroscopic level siphon into virtually identical biological characteristics that appear on the molecular level. One such characteristic are nucleotides. Nucleotides are essential biomolecules due to their imperative role in energy transfer, metabolism, intercellular signaling, and much more (1). Plants and animals alike depend on nucleotides for development and metabolism, yet the mechanisms for maintaining pools of nucleotides differ. As a result, biosynthetic pathways have evolved to regulate the synthesis and degradation of nucleotides. Dysfunctional regulation of nucleotide biosynthesis pathways results in disastrous disorders within an organism. Yet the most imperative of these is inhibition of DNA regulation, which can impede an organism's life.

Nucleotide structure

Nucleotides are composed of a nitrogenous base linked to ribose or 2 - deoxyribose, through an amide linkage on carbon 1 (Figure 1). The sugar can link one, two, or three phosphate groups on carbon 4 or 5 to create nucleoside mono, di, or tri phosphate. These phosphates are designated as the alpha, beta, and gamma. The presence of a phosphate results in a nucleotide, whereas the absence of the phosphate results in a nucleoside (2). In order to differentiate the numbering between the carbons on the
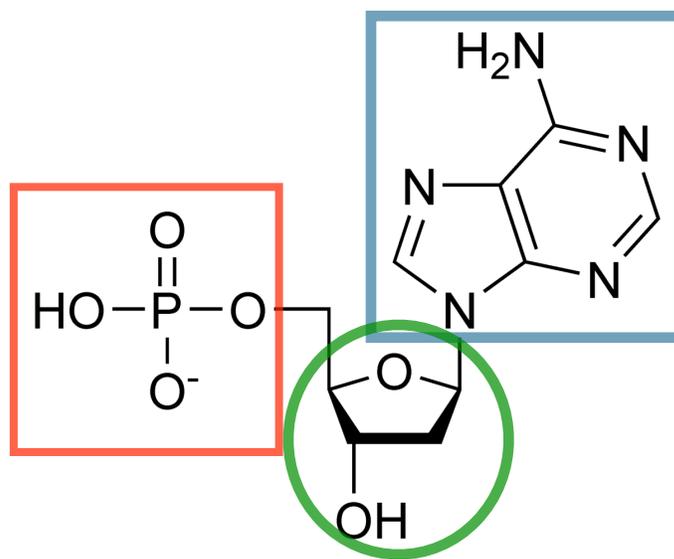
Figure 1| Nucleotide structure The basic nucleotide structure is compromised of a pentose ribose or 2'-deoxyribose sugar (green), a nitrogenous base (blue), and a phosphate group (red).

nitrogenous base and the carbons on the sugar, a prime system is utilized. The carbons on the nitrogenous base are numbered one through nine and the carbons on the sugar are numbered one prime through five prime.

Deoxyribose lacks a hydroxyl group on either the 2' or 3' carbon. Conversely the ribose maintains hydroxyl groups on both 2' and 3' carbon (2). The nitrogenous bases are planar, aromatic, and heterocyclic. These features drive the structure and function of biomolecules such as deoxyribonucleic acid (DNA) and ribonucleic acid (RNA). Nitrogenous bases are further subdivided into two structural derivatives, purines, and pyrimidines (Figure 2).

The most common purines found in nature are adenine (A) and guanine (G) and nature's most common pyrimidines are cytosine (C), thymine (T), and uracil (U). Uracil is selectively incorporated into ribonucleic acid (RNA) but not DNA (3). Nucleosides
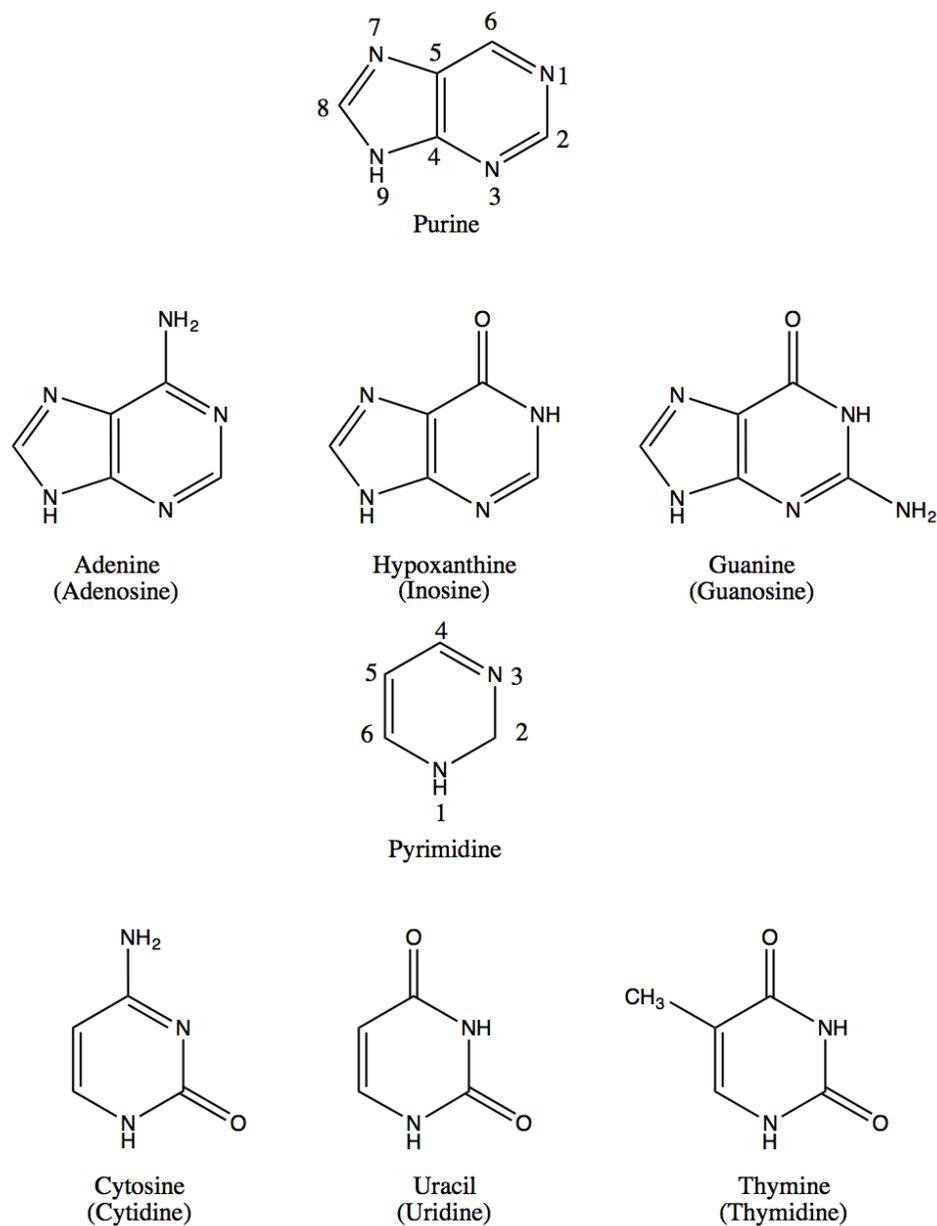
Figure 2| Purine and pyrimidine The purine ring is composed of two fused rings. Pyrimidines have one ring. The most commonly found purine and pyrimidine bases are listed above with the corresponding nucleoside in parenthesis (35)

such as adenosine are utilized in various functions of an organism. Adenosine triphosphate (ATP) can be hydrolyzed to adenosine diphosphate (ADP) to release 35 kilojoules per mol of energy (2). Many biochemical reactions must be coupled with ATP

hydrolysis in order for the reaction to be more thermodynamically favorable. An example, the light independent reactions in photosynthesis consume 9 molecules of ATP in order to convert carbon dioxide to glucose. Glucose is then utilized by plants as food. If this reaction does not couple ATP hydrolysis to it, it simply would not occur. By extension the plant would die due to lack of food.

Purine synthesis pathway

In 1948, John Buchanan identified the mechanism of purine synthesis. Buchanan isotopically labeled compounds and fed the compounds to pigeons. Once the pigeons excreted uric acid, Buchanan was able to determine the position of each labeled atom. Nitrogen 1 (N1) is derived from the amino acid aspartate. N3 and N9 come from the amide functional group from the glutamine amino acid (5). The amino acid glycine is intrinsically incorporated as C4, C5, and N7 (4) (Figure 3). Formate is included as C2 and
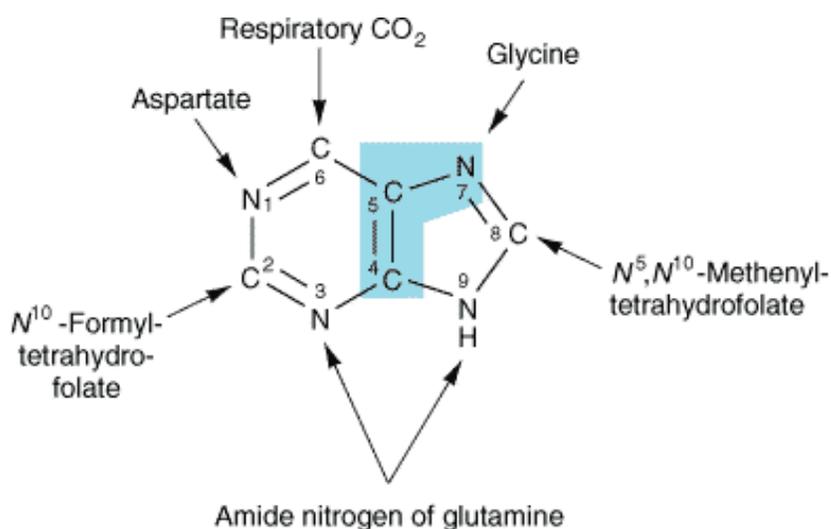
Figure 3| Glycine formation Purine structure and corresponding sources of atoms as outlined by John Buchanan (4).

C8, and bicarbonate forms C6. Buchanan later teamed with researcher G. Robert Greenburg to elucidate the purine synthesis pathway. The key facet Greenburg and Buchanan revealed is "purines are identically formed as sub nucleotides rather than as free bases" (5). Thus organisms ranging from paramecium to protozoa have nucleotides that are synthesized identically. Ten reactions that are catalyzed by multiple enzymes result in the purine precursor, inosine monophosphate (IMP). Key steps within the pathway are summarized below (6).
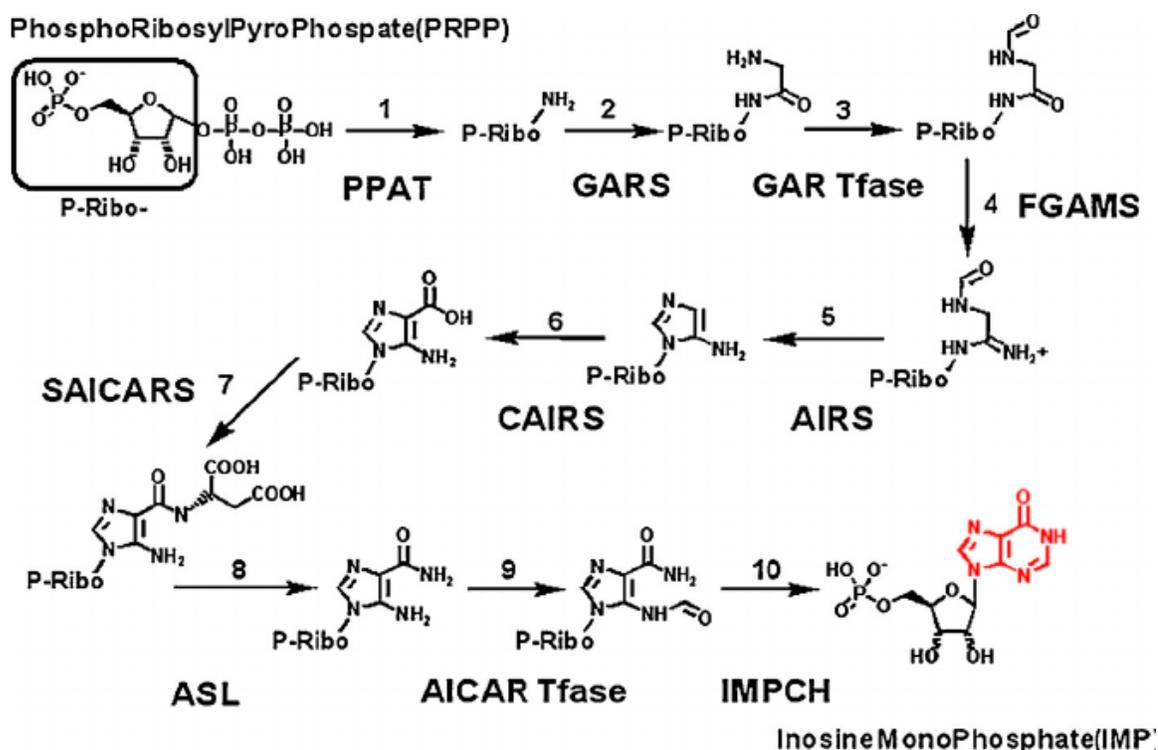
Figure 4 | Purine biosynthesis pathway occurs in 10 steps. The precursor material, pentose is converted to inosine monophosphate. The addition of N3 in step seven is an energetically costly step that often results in plants recycling purines rather than generate new ones. Reprinted with permission from Science Direct (7)

Step 1:   The ribose ring is activated by reacting with adenosine triphosphate to

form 5- phosphoribosyl-alpha pyrophosphate (PRPP). PRPP can diverge

from continuing in the purine synthesis pathway to serve as starting

material to generate the amino acids histidine and tryptophan. As a result,

this step must be tightly regulated in order to maintain cellular

concentrations of purines and amino acids (Figure 4).

Step 2:   Phosphates are hydrolyzed to invert the alpha configuration of C1 on

PRPP to generate the anomeric form. Glutamine's amide group

displaces the original pyrophosphate group and begins the synthesis of

the nitrogenous base (Figure 4).

Step 3:   N7, C3, and C5 are added to the substrate via an amide linkage of

glycine's carboxyl group. (Figure 4)

Step 4:   C8 is added by the formation of the alpha amino group (Figure 4)

Step 5:   N3 is added to the ring by the amino group of another glutamine.

Aromatization of the indole ring is a result of the tautomeric shift from

imine to enamine (Figure 4).

Step 7:   The addition of N3 is facilitated by the enzyme AIR carboxylase.

            Plants have two isoforms of AIR carboxylase to promote this reaction,

            PurE and PurK. PurE can add N3 to the ring but requires a high cellular

            concentration of 110 mM bicarbonate for this reaction to occur. PurK can

            facilitate PurE to lower the required concentration of bicarbonate, but

            must use a large amount of ATP in exchange. The high cost in energy to

            perform this step can result in plants utilizing other means to generate

            purines. Afterwards an amide-forming condensation reaction adds N1

            from an aspartate followed by the addition of C2 by formylation (Figure

            4).

Step 10:   Cyclization of IMP occurs through the elimination of water. This last

            step is energetically favorable as it does not require the hydrolysis of

            ATP.

De novo purine biosynthesis

De novo purine biosynthesis pathway is highly conserved among all organisms.
Yet key steps within the pathway are energetically unfavorable, and thus the organism
may rely on the purine salvage pathway. "In contrast to the *de novo* purine nucleotide
synthetic pathway, which is virtually identical in all cells, salvage pathways are diverse in

character and distribution" (5). Purines are recycled by either adenine phosphoribosyltransferase (ARPT) or hypoxanthine-guanine phosphoribosyltransferase (HGPRT). ARPT catalyzes the breaking of the glycosidic bond of adenosine monophosphate to generate adenine. Adenine can also be generated from nucleotides and adenosine deaminase (ADA) (5). Deaminases catalyze the removal of an amine group. ADA specifically binds to adenosine and converts the amine on C6 to generate a
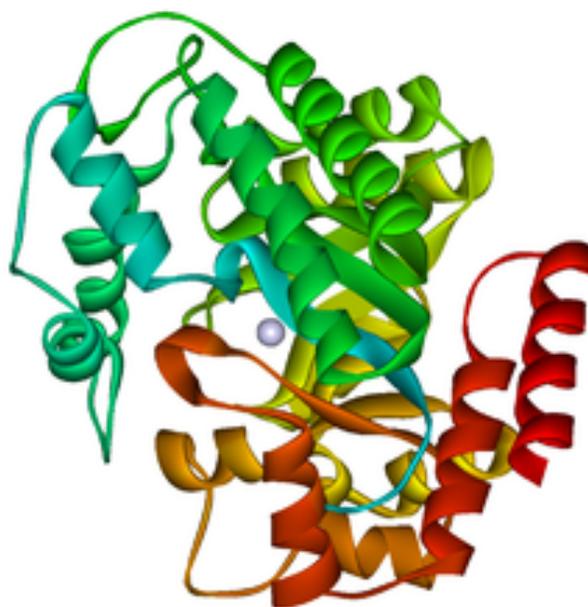
Figure 5 | **The structure of adenosine deaminase** (ADA) in ribbon format crystallized from Bos taurus. (Protein Data Bank entry : 1VFL). Structure rendered from protein data bank in Pymol (44).

carbonyl, resulting in inosine.

Adenosine deaminase (ADA)

Adenosine deaminase (8) is an eight stranded alpha beta barrel mix hydrolase. The amino acid sequence of ADA is highly conserved among a vast variety of organisms.

It is characterized by 356 amino acids and a total molecular weight of 40,407.45 Daltons (Figure 5). Similar to other alpha/beta barrel mix proteins, the active site resides towards the carbon terminal end of the beta barrel. Although a tryptophan (amino acids 117 and 161) resides around the active site of the protein, it doesn't directly participate in the enzymatic reaction. However it does aid in generating fluorescence when the active site binds a substrate (9). ADA can adopt an open form, lacking a bound substate, and a closed form when bound to a substrate. The conformational change to the closed form of ADA results in a phenylalanine (amino acid, 65) moving over the substrate binding pocket. The conversion of the open form to the closed form is driven by a water molecule at a key binding position (10). A zinc ion is buried inside the catalytic domain of the enzyme (Figure 6).

ADA's gene has been isolated, sequenced, and evaluated from human, S*accaromyces cerevisiae* (42)*,* bovine (43), and *Plasmodium yoelii* (9)*.* The homology between different isoforms of ADA among species is very high. Moreover the overall enzymatic mechanism is conserved as well.

Mechanism of enzymatic activity of adenosine deaminase

The mechanism of the conversion of adenosine to inosine occurs in two key parts (9). First, a hydroxyl group is added in a stereospecific manner to carbon 6 to generate a tetrahedral intermediate. This is followed by the elimination of ammonia to generate inosine. Zinc ions are important in the catalytic domain because they help activate the
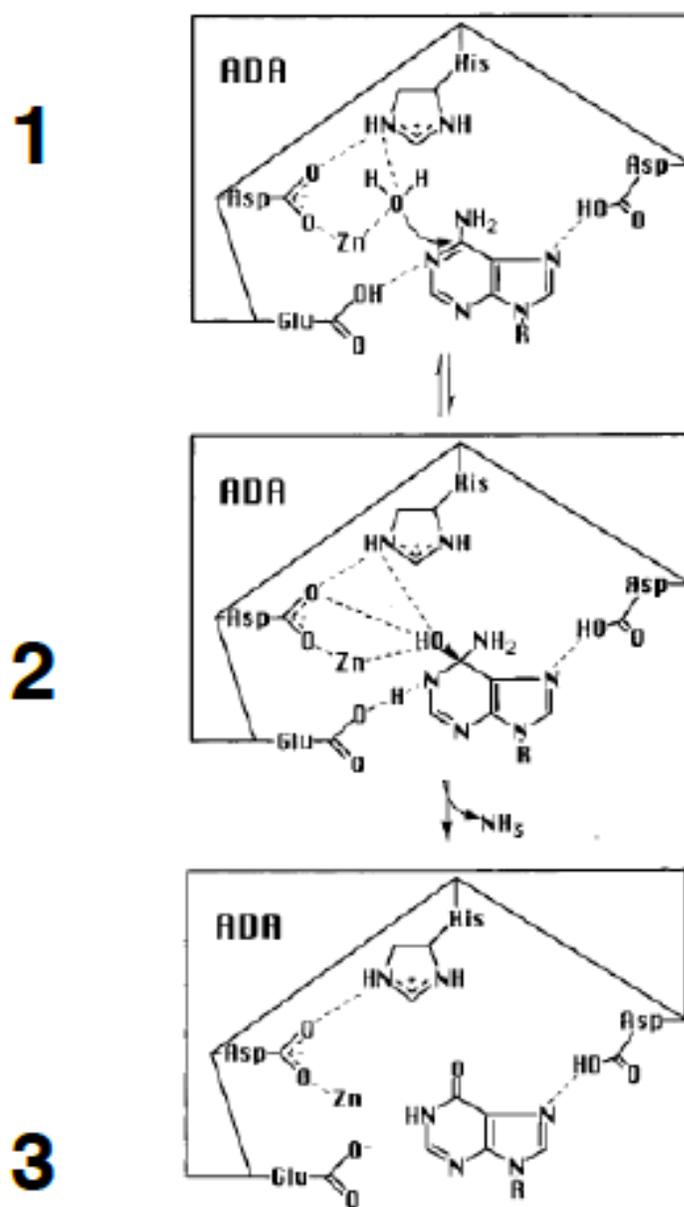
Figure 6 | Reaction mechanism of adenosine deaminase converting adenosine to inosine through a 3 step process: Zinc (Zn) activating water, intermediate coordination, and ammonia release. **[1]** describes the coordination of the adenosine substrate binding to the active site pocket of adenosine deaminase. Zn activates the water molecule as the water is coordinated through histidine, aspartic acid, and glutamic acid. The water performs a nucleophilic attack on the amide on the adenosine. **[2]** shows the transition state after the nucleophilic attack and before the release of ammonia. **[3]** shows the final product of inosine still coordinated with the aspartic acid residue. The exact mechanism on how this final step occurs is still unknown. (9) Reprint with permission from John Wiley and Sons.

water molecule to generate a better nucleophile. Moreover the zinc ion helps position adenosine in the active site. Nitrogen 1 on adenosine hydrogen-bonds to the glutamic acid residue. As a result nitrogen 1's double-bond character is decreased and promotes a nucleophilic attack on carbon 6. A histidine residue aids in stabilizing the hydroxyl nucleophile (Figure 6). A carboxyl group from a neighboring aspartic acid aids in orienting the hydroxyl group. The hydroxyl group is then positioned to attack carbon 6, thus generating a tetrahedral intermediate (Figure 6). The final step dismantles the tetrahedral intermediate and eliminates ammonia (Figure 6). Unfortunately the exact mechanism of the final step has not been fully described.

Nucleoside hydrolases (nucleosidases)

Nucleoside hydrolases or nucleosidases also serve an important role in the purine salvage pathway. They have been isolated and identified in various bacteria (12), yeast (13), protozoa (14), and more. These enzymes hydrolyze the N-glycosidic bond of ribonucleosides to generate a nitrogenous base and ribose. Nucleosidases were classified into 3 classes on the basis of substrate preference: inosine-uridine preferring nucleoside hydrolases (IU-NH), purine specific inosine-adenosine-guanosine preferring nucleoside hydrolases (IAG-NH), and 6 oxopurine specific inosine-guanosine preferring nucleoside hydrolases (IG-NH). (15). However this three tier system has become archaic as more nucelosidases have been identified that do not fit perfectly within any of the listed categories. Traditionally IU-NH exhibit a homotetramer structure whereas IAG-NH exist

as a homodimer. All sequenced nucleosidases retain the DXDXXXDD amino acid motif at the N-terminus.

Mechanism of ribosyl hydrolysis

Although a wide variety of nucleosidases vary in nucleoside preference, ribose is the hallmark minimum requirement for substrate recognition. (15). The active site for nucleosidases is buried deep inside the subunit where the ribose is coordinated with 8 amino acids and a calcium ion. Ribose coordination among the varying amino acid differs between IU-NH and IAG-NH. Yet the proposed mechanism for both classes of nucleosidases suggests ribose hydrolysis is a SN-1 reaction with a oxocarbenium ion-like transition state being adopted (Figure 7). A combination of three strategies have been proposed for the a mechanism of purine hydrolysis: 1. steric and electrostatic stabilization generated from the ribosyl ring absorbing a substantial positive charge 2. activation of the nucleophile, water, through a calcium ion 3. leaving group activation by the protonation of N-7, which destabilizes the N-glycosidic bond by decreasing the electron density in the purine ring. (16).

Inosine nucleosidases

Inosine nucleosidases have been isolated and identified in *Azotobacter vinelandii* (17) and the plant yellow lupin (18). Inosine nucleosidase isolated from yellow lupin has a molecular weight of 62 kDa and an optimum pH 8 (18). The highest activity

(a)

Figure 7 | Ribose hydrolysis is characterized by a combination of 3 strategies that promote hydrolysis : 1. steric and electrostatic stability of the ribose ring. 2. activation of the nucleophile, water 3. leaving group activation via protonation of N-7 of the purine ring. This reaction is proposed to proceed through an SN-1 mechanism with an oxocarbenium ion-like transition state. Reprint permission from Elsevier (15).

was observed in 6 day old germinated seedlings with an inosine Micahelis constant, K_m of 65 μM. *Azotobacter vinelandii* inosine nucleosidase has a molecular weight of 70 kDa and inosine K_m of 0.65 mM at the optimum pH 9 (17). The isolated enzyme had a "strict substrate preference towards nucleosides without amino groups in the purine moiety (18)." Moreover, adenine and hypoxanthine acted as inhibitors to enzymatic activity.

Nucleosidases have been isolated from other sources such as insects, protozoa, plants, and yeast that have less stringent substrate binding affinities beyond their target substrate that are inclusive of substrates like inosine. For example, adenosine nucleosidase isolated from Jerusalem artichoke shoot (19) exhibited activity with adenosine, inosine, and guanosine. The optimum pH for all three substrates ranged from 5 to 7. The K_m for adenosine, inosine, and guanosine were 17 μM, 2.5 μM, and 8.5 μM respectively. Nucleoside hydrolases isolated from *Crithidia fasciculata* (20) had a native molecular weight of 143 kDa and a subunit molecular weight of 34 kDa. The hydrolase isolated had a wider substrate affinity for inosine, guanosine, uridine, and more. (20)

The varying substrate affinity among the different nucleosidases provides insight on how the different purine substrates bind to the active site of the enzyme. Two active sites have been modeled for IU-NH and IAG-NH. Figure 8 displays the active site for IAG-NH of *Trypanosoma vivax* with inosine bound in complex (15). Ribose is complexed with 8 amino acids and a calcium ion coordinated with Asp10, Asp15, and Asp261 side chain oxygen, and Thr137 main chain carbonyl. The nucleobase is bound to the active site within a hydrophobic pocket parallel stacked between two tryptophan

residues. It is inferred that the purine specificity is driven by the pi-pi stacking "sandwich" (15).

Figure 8| Inosine bound in nucleosidase active site is modeled by the IAG-NH from *Trypansoma vivax*. Reprint with permission from Elsevier (15).

ADA purification strategies

Adenosine deaminase was first partially purified by George Brawerman and Erwin Chargaff in 1954 from commercial malt diastase (21). Brawerman and Chargaff studied the degradation of DNA and realized the nucleosides remained intact. Along with phosphomonoesterase, their work deduced the existence of the enzyme adenosine deaminase (21). Their partial purification of adenosine deaminase resulted in a guiding purification technique that has been adopted and enhanced by researchers. Three key published strategies have served as a guiding reference in developing the purification of the deaminating nucleosidase from the *Pisum sativum* (Alaksa pea). The final result of each purification is summarized in Table 1 below.

Table 1|Adenosine deaminase was purified from mice and plasmodium using a three step purification protocol building from Brawrman and Chargaff's partial purification (21). The enzymatic activity of the purified ADA can be compared by the specific activity. The specific activity is calculated by the conversion of adenosine to inosine (Giusti 1974) per mmol of ADA per minute.

Expression Source	Total purified protein (mg)	Specific Activity (mmol/min*min)	Percent recovery %	Research group
Fastiola gigantica	0.43	63.7	35.7	Ehab M.M. Ali (22)
Plasmodium yoelli	2.92 (mg/mL)	1.7646	47.1	Banerjee (23)
H. dromedari	0.63	150.8	31.6	Mohammad (24)

Rudra Prasanna Banerjee's research group proposed a three step ADA purification technique from plasmodium infected swiss mice (23). Banerjee selected a balanced two step ammonium sulfate precipitation as the beginning purification step. This step was effective in generating purification of the protein as the specific activity moderately increased from 0.1797 to 0.1973 units per micrograms of enzyme with minimal loss in protein concentration. A DEAE weak anion exchange column followed after gentle dialysis from the precipitation step. Banerjee applied a more basic pH (7.5) to elute the protein in a buffer at physiological pH. A stepwise sodium chloride salt gradient eluted ADA from the column from 0.1 M to 0.4 M NaCl. Sephadex G-100 was the standard final step in protein purification to generate a "monomeric protein with the molecular weight of 41 kDa."

Ehab M.M. Ali's research group selected sheep liver infected with *Fasciola gigantia* plasmodium (22) to purify ADA. Instead of an ammonium sulfate precipitation, Ali's group used acetone precipitation as the initial separation step. Ali pelleted the precipitated protein and redissolved it in sodium phosphate buffer. Ali mirrored Banjeree in utilizing a weak anion exchange column after precipitation. "CM-cellulose produced a number of proteins as well as two peaks of ADA activity, (these) fractions were designated as ADA I and II, respectively." Ali chose to further purify the second isoform of ADA because of its higher activity. In the final step, Ali utilized gel filtration chromatography using a Sephacryl S-2100 column for ADA II. An analysis by 10% SDS-PAGE gel showed a single band with a molecular weight of 29 kDa. The optimum pH for

the purified ADA II was 7.5. ADA II showed activity with the substates adenosine, 2'

deoxyadenosine, and guanosine.

Tarek M. Mohamed's research group purified ADA from *H. dromedarri* (tick

eggs) (24). Mohammed performed an acetone extraction similar to Ali, yet dialyzed the

precipitated protein in 50 mM sodium potassium phosphate buffer, pH 7.5 overnight

against 50 mM sodium acetate buffer pH 5.5. Mohammed utilized a DEAE column in a

similar manner as Ali, but performed a linear gradient from 0-0.5 M sodium chloride.

Mohammed's DEAE elution profile showed four peaks: a wash peak, two low salt peaks

(roughly around 0.1 M NaCl), and broad peak in the middle of the gradient (0.2 M NaCl).

These peaks were labeled ADA I, II, and III; the two low salt peaks were combined and

concentrated to yield ADA II, the most active fraction. ADAII was purified further by gel

filtration on a Sephacryl S-200 column. Mohammed estimated their purified ADA

molecular weight was 42,000 Daltons which was confirmed by SDS-PAGE.

CHAPTER II

MATERIALS AND METHODS

Equipment and instrumentation

Protein fractions were separated and purified using a GE AKTA Purifier Fast Protein Liquid chromatography systems with the GE Unicorn software. The chromatography columns, Mono Q 26/10, Superdex S200 (26/10), and Sephacryl S100 (26/10) were provided by GE as well. Enzymatic activity was observed using Dionex Ultimate 3000 High Performance Liquid Chromatography (HPLC) equipped with a multi-wavelength UV detector. SDS-PAGE and Native-PAGE was performed using a Bio-Rad electrophoresis instrument..

Materials and Reagents

The germinated seeds utilized were (20 g) Arevejas wilt resistant breed of Alaska pea seeds from Ferry-Morse Seed Company. Ammonium phosphate and methanol were purchased from Fisher Scientific at HPLC reagent grade. All other reagents to make buffers were purchased from Fisher at reagent grade purity. Nucleosides utilized for enzymatic analysis were purchased from Sigma-Aldrich. The protamine sulfate from salmon, protease inhibitor for plants, and all proteins comprising of the size exclusion protein standards were obtained from Sigma-Aldrich. The protein dialysis was performed using dialysis tubing from Fisher Scientific. The protein samples within each step of purification were concentrated using Amicon Ultra-15, 10 and 50 mL, concentrator.

Samples were then filtered using a Millex low protein binding durapore filter. The protein concentration for each sample was performed using Bio-Rad assay standard and bovine serum albumin. Polyacrylmide gels were Lonza Precast 4-12% Tris-Glycine gradient gels. A Precision Plus unstained protein standard and 10x Tris-Glycine-SDS running buffer from Bio-Rad were utilized.

Protein extraction

In order to prevent contamination, the seeds were sterilized with bleach. One 20 gram packet of Alaska pea seeds were washed with 75 mL of bleach with occasional stirring for 3 minutes. Afterwards the seeds were thoroughly washed and rinsed with tap water for ten minutes. Imbibition was promoted by placing the sterilized seeds between two damp paper towels within a container filled with 20 mL of tap water. The seeds were checked daily to ensure no contamination was present. Four days after sterilization the seeds were fully germinated and were prepared for extraction. If extra time was needed between the final germination and extraction, then the seeds were stored at 4°C to slow down cellular respiration to prevent further germination. The mass of the germinated seeds was referred to as "wet mass."

The volume of extraction buffer used was 1:5 (w/v); consisting of the ratio of seed wet mass to buffer volume. The extraction buffer contained 50 mM Tris (formally known as Tris Base) pH 7.4, 1 mM dithiothreitol (DTT), 2% (w/v) protamine sulfate, and roughly 5 mg protease inhibitor cocktail for plant tissues. The buffer was created either

on ice or at 4°C to minimize buffer pH fluctuations. The extraction was performed at 4°C as well.

The germinated seeds and half of the extraction buffer were combined in a blender and homogenized for 1 minute. The sample was then filtered by a double layer cheesecloth into a cold beaker. Afterwards, the sample was centrifuged at 30,000 xg for thirty minutes. The supernatant was collected and a 50 μL aliquot saved. The cell pellet was combined with the remaining volume of extraction buffer. The subsequent steps were repeated as stated above and the two cell supernatants were combined to form the clarified lysate.

Ammonium sulfate precipitation

An ammonium sulfate precipitation ("salt out") followed the cell extraction. The clarified lysate went through a two step ammonium sulfate precipitation, 0-35% and 35-70% (w/v). Each precipitation step was performed either on ice or at 4°C. The ammonium sulfate was slowly added and stirred into solution. After the ammonium sulfate was added, the sample was slowly stirred.

The 0-35% was stirred for 4-5 hours, while the 35-70% step was stirred overnight at 4°C. After the allotted time for mixing was completed the sample was centrifuged at 25,000 xg for 40 minutes. The pellet of the 35-70 % step was dialyzed against 1L of 50 mM Tris 1mM DTT pH 7.4 buffer overnight. The buffer was changed three times during this period.

Mono Q ion exchange chromatography

The dialyzed sample was centrifuged at 25,000 xg for 5 minutes to pellet any debris. All buffers and samples applied to the FPLC were filtered to prevent clogging of the instrument. If the total volume of the centrifuged sample was greater than 5 mL, then multiple runs of the Mono Q ion exchange column were required.

The Mono Q column was equilibrated with the starting buffer, buffer A, consisting of 50 mM Tris 1 mM DTT pH 7.4 for two column volumes (CV). A Mono Q FF 16/10 column with a CV of 20 mL was utilized. Five mL of the centrifuged sample was applied to Mono Q column followed by a wash step for 2.5 CV.

The target protein was eluted from the Mono Q column using a stepwise gradient of increasing sodium chloride salt. The eluting buffer, buffer B consisted of 50 mM Tris 1 mM DTT 1 M NaCl at pH 7.4. The gradient consisted of 0.100, 0.125, 0.150, 0.200, 0.250, and 0.600 M NaCl. Each gradient step eluted for 2.5 CV to collect 10 mL fractions at a flow rate of 3 mL per minute.

Upon completion of the gradient, the Mono Q column was washed with 2 M NaCl for 2 CV and rinsed with deionized 18 MΩ water for 5 CV. Eluted peak fractions were pooled and analyzed for the rate of adenosine depletion through conversion of adenosine to product using HPLC. Subsequent fractions displaying high enzymatic activity and with the target protein molecular weight were concentrated to 4 mL using an Amicon Ultra-15 50 mL concentrator.

Size exclusion chromatography

The 4 mL concentrated sample was centrifuged at 25,000 xg for 5 minutes to pellet any precipitate or debris, then loaded onto the Superdex 26/60 S200 FPLC size exclusion column. The column was equilibrated with a filtered buffer of 100 mM Tris 300 mM NaCl pH 7.2 for one column volume (318 mL) at a flow rate of 0.5 mL per minute. After column equilibration, the sample eluted in 1.5 column volumes at a flow rate of 0.5 mL/min. The fraction containing the target protein was concentrated to 3 mL using an Amicon Ultra-15 50 mL concentrator.

Determination of protein concentration (Bradford assay)

A standard curve of the bovine serum albumin (BSA) was prepared at the concentrations of 0.000, 5.000, 10.00, 15.00, 20.00, and 25.00 μg/μL (28). Dilutions were generated using DI water. The 1.47 mg/mL stock solution of BSA was diluted to 0.500 mg/mL. This was then utilized to make subsequent dilutions of the above standard concentrations to a total volume of 800 μL. Two hundred μL of Bio-Rad protein assay dye was added to the 800 μL of the BSA protein standard. The solution was vortexd and incubated for 5 minutes. The spectrophotometer was set to 595 nm wavelength and equilibrated for 10 minutes. The spectrophotometer was blanked (standardized to 0% absorbance) with the 0.000 μg/uL BSA standard. Each BSA standard absorbance was measured and recorded. A 50 μL aliquot of a protein sample was mixed with 750 μL of DI water, 200 μL of Bio-Rad protein dye, and incubated for 5 minutes. The preceding

step was repeated for every sample of each step in the protein purification protocol. The absorbance was measured and recorded. A linear regression of the absorbance versus the BSA protein concentration was calculated. If the protein samples's absorbance was below or above the absorbance linear range of the BSA standards, then the protein sample was concentrated or diluted until the absorbance was within the linear limits. The protein concentration of each measured aliquot was calculated from the BSA standards linear regression.

Determination of adenosine enzymatic activity by HPLC

The enzymatic activity of various fractions was determined by the measured rate of depletion of adenosine from a starting concentration. A reverse-phase Phenomenex Hypersil C18 (4.6 x 50 mm) column was utilized on the HPLC to separate and analyze reaction products. An adenosine reaction mixture consisting of 1 mM adenosine in 50 mM Tris pH 7.2 standard was filtered. A 900 μL aliquot of reaction mixture was added with 100 μL of an enzyme sample into a HPLC vial. The time the enzyme was added was recorded. The preceding step was repeated for every aliquot for every step in the protein purification protocol. Each sample vial was analyzed on the HPLC for 15 minutes at a flow rate of 0.600 mL/min with the mobile phase of 98% 10 mM ammonium phosphate buffer pH 5.2 and 2% HPLC-grade methanol at a 254 nm wavelength. The enzymatic activity of each sample was analyzed by a linear regression of the rate of decrease in area of adenosine versus the time elapsed in hours.

Determination of native molecular weight

A protein standard was generated by combining commercially purified proteins in 4 mL of 50 mM Tris pH 7.2 buffer. Five mg of Blue Dextran, carbonic anhydrase, hemoglobin, alcohol dehydrogenase, beta amylase and cytochrome C were combined. The protein standard was filtered and loaded onto the Superdex 200 size exclusion FPLC column. The Superdex 26/60 S200 column was equilibrated for one column volume (318 mL) with the filtered buffer of 100 mM Tris 300 mM NaCl pH 7.2. The proteins were eluted from the column at a flow rate of 0.5 mL per minute for 1.5 column volumes. A calibration curve was generated from a semi-log plot of the protein standard's molecular weight versus elution volume (29). The molecular weight of the purified enzyme was calculated by applying its retention volume to the linear regression equation.

Determination of oligomerization state

A 12% native electrophoresis gel and running buffer was adapted from the protocol outlined in "Gel Electrophoresis of Proteins" (30). Fifty μL of the purified deaminating nucleosidase enzyme was aliquoted into 5 tubes. Each tube was labeled " 0, 5, 15, 30, 60, 90" according to the time interval, in seconds, each tube was to be incubated at 75 °C (31). Each sample then received 50 μL of cold sample buffer and loaded onto the native gel and run for 3 hours at 120 voltage in a 4 °C. The gel was then stained with Coomassie blue to visualize the bands.

Determination of optimum pH

A universal buffer (32) was made consisting of 33 mM citric acid, 33 mM phosphoric acid, and 1 % w/v boric acid in 1M sodium hydroxide. The buffer was adjusted to the desired pH before diluting the buffer with DI water to reach desired the final volume. A 1mM adenosine reaction mixture was generated in the designated pH buffer. Reaction mixtures were created at 0.5 pH intervals from 3 to 9. Nine hundred and seventy five µL of 1mM adenosine reaction mixture and 25 µL of enzyme were combined in a 1 mL HPLC vial. The activity was measured and analyzed using the techniques outlined in the preceding section: Determination of enzymatic activity by HPLC. This assay was repeated using inosine instead of adenosine as the substrate.

Michaelis-Menten kinetic analysis of inosine

The Michaelis-Menten constant, Km, for the substrate inosine was determined by varying the concentration and calculating the reaction activity or velocity (33). The varied inosine concentrations, were 25, 50, 100, 250, 500, 750, and 1000 µM. The reaction was carried out in Teorell-Stenhagen universal buffer pH 6. The respective substrate concentration standard was combined with 50 µL of purified enzyme for a total reaction volume of 1 mL and analyzed by HPLC. The velocity of the reaction was determined by the measured area decrease of inosine as a function of time. A Michaelis-Menten plot was created by plotting velocity versus inosine substrate concentration. The

Km and maximum velocity, Vmax, were determined from the double reciprocal Lineweaver-Burk plot.

CHAPTER III

RESULTS AND DISCUSSIONS

Purification of adenosine deaminating nucleosidase

One packet of twenty grams of Alaska Pea seeds was germinated on a damp paper towel for four days until the cotyledon was exposed. "Germination commences when the dry seed takes up water (imbibition) and is completed when the embryonic root visibly emerges through the outer structures of the seed (24)." The final seed mass was roughly four times the dry seed mass. A 5:1 (w/v) extraction buffer was utilized as "better extraction is obtained with a higher ratio of buffer volume to fresh tissue weight (25)." The seeds were blended for total pod destruction for 30 seconds on and off for 2 minutes. This prevented excessive frothing that denotes protein denaturation. The lysate was centrifuged to remove cellular debris and extract the total protein into the supernatant.

An ammonium sulfate precipitation followed to concentrate the protein. This step was selected as a salting out can achieve a purification factor of 3-5 while maintaining a percent recovery of 70% or greater. Moreover, the sample protein was concentrated as the salt concentration increased (26). The maximum saturation was increased to 70% achieved in two steps, 0-35% and 35-70%. The ammonium sulfate was added slowly as rapid stirring of large volumes of the salt stirred in a time resulted in bubble formation indicative of protein denaturation. The target protein was pelleted by centrifugation and

dialyzed in buffer A to eliminate the ammonium sulfate salt in preparation for ion exchange chromatography.

An anion exchange column was utilized following salting out precipitation. In previous purifications of nucleosidases and deaminase (22, 23) a DEAE column was selected with a sodium phosphate buffer at pH 7 using a step wise increasing salt gradient. This ion exchange purification was attempted using DEAE 16/10 FF column using the elution principals above. The subsequent chromatograph is shown in Figure 9. The DEAE ion exchange column resulted in inefficient separation of the target protein from the larger sample. This was evident as the target protein eluted from the column in multiple fractions. Also as the DTT degraded in the buffer over the dialysis period, the target protein did not bind as tight to the column. As a result the protein eluted in the wash step. Moreover, the fatty seed material from the concentrated dialyzed sample required a 2M NaCl to elute the residual protein off of the DEAE column. If this final elution step was not included, the ion exchange column would clog causing the FPLC system pressure to rise.

In order to increase the selectivity of the target protein binding to the Mono Q column, the buffer was changed to Tris-Base. Tris results in less temperature dependent pH fluctuations than potassium phosphate and has an overall pKa, 8.1, (27) closer to the desired pH of the Mono Q buffer. The buffer pH was shifted from 7 to a more basic 7.5. When the dialysis buffer was at pH less than 6, the protein sample turned a bright pink color; whereas adjusting the buffer pH greater than 8, resulted in the sample turning a
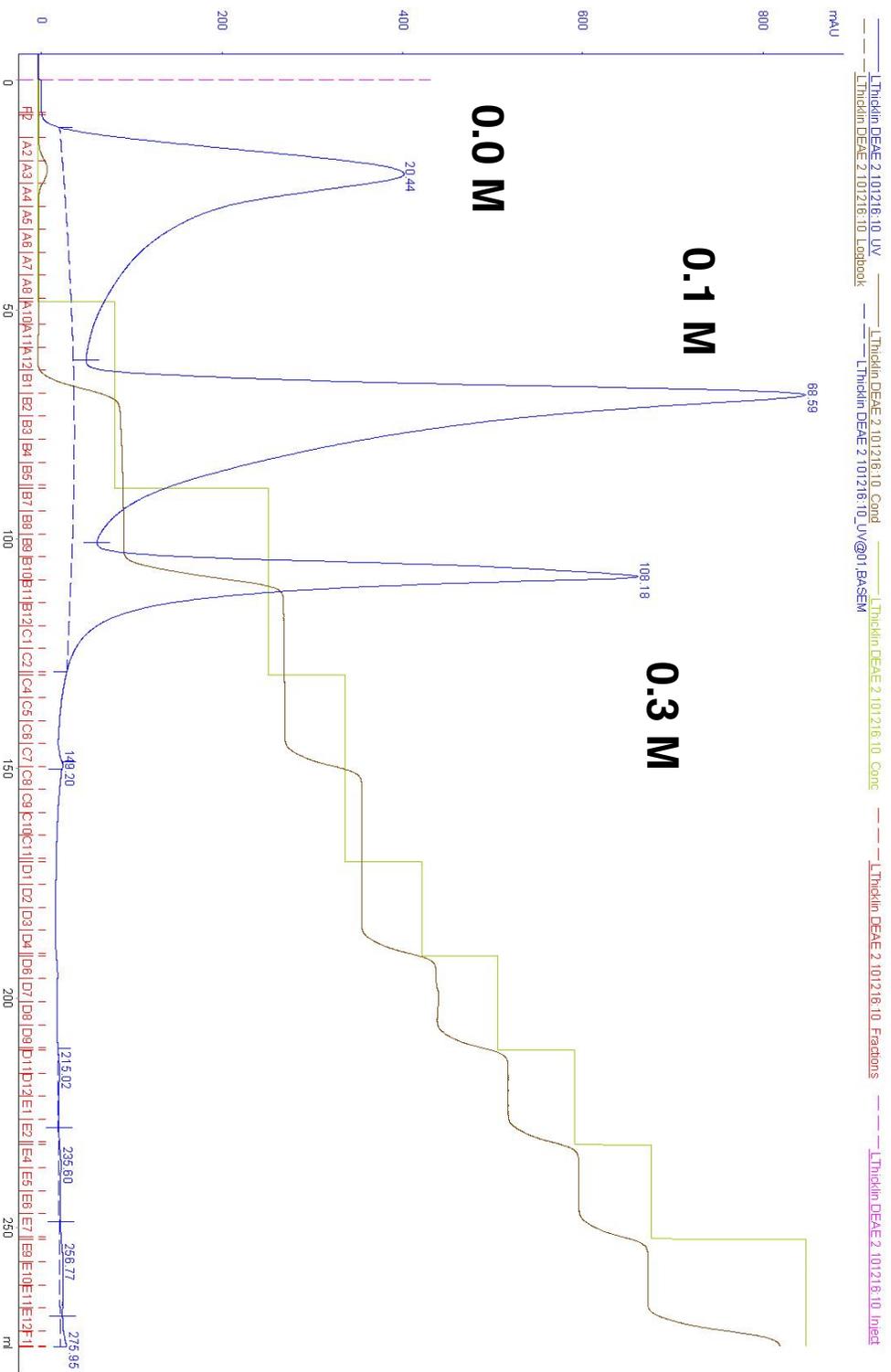
Figure 9 | The DEAE chromatogram with a load volume of 5 mL. Each step is 2 column volumes (20 mL=1CV), for 9 steps total at a flow of 3 mL/minute. The steps were 0, 10, 30, 40, 50, 60, 70, 80, and 100% Buffer B. Buffer A: 50 mM Tris 1 mM DTT pH 7.45 Buffer B: 50 mM Tris 1 mM DTT 1M NaCl pH 7.5 at a flow rate of 3 mL per minute. Each eluted fraction was 10 mL. Two M NaCl was required to elute the remaining protein.

golden yellow color. This would be indicative of a metal co-factor bound in the protein changing oxidation state. In both adenosine deaminase and nucleosidase, a metal cofactor is bound deep in the active site; zinc and calcium ions respectively.

The Mono-Q column and the subsequent buffer and elution changes (Figure 10) resulted in more protein binding to the column compared to the DEAE column (Figure 9). This is evident by less eluting protein in the wash step and more targeted elution of the desired protein in the 0.100 M step. The two prominent peak fractions at steps 0.1 M and 0.6 M NaCl were pooled and tested for adenosine product activity using HPLC. Both of these fractions contained activity, yet the 0.1 M pooled fraction was more active. Also the SDS-PAGE of the pooled fractions (Figure 12) revealed the 0.1 M pooled fractions contained two bands at 100 kDa and 20 kDa. Thus the 0.1 M pooled fractions were selected for further purification.

The final purification step was size exclusion chromatography. The two prominent bands in the 0.1 M step pooled fraction were best separated by size rather than using a hydroxyapatite column because the protein shared similar binding properties and enzymatic activity. In order to maximize the separation and increase purity of both proteins, the Superdex S200 column was utilized at a flow rate of 0.5 mL/min. A slower flow rate increased the retention time of smaller proteins thus widening the separation between the 100 kDa and 20 kDa proteins (Figure 11). This strategy was successful as two prominent peaks were resolved, pooled, and labeled adenosine deaminating
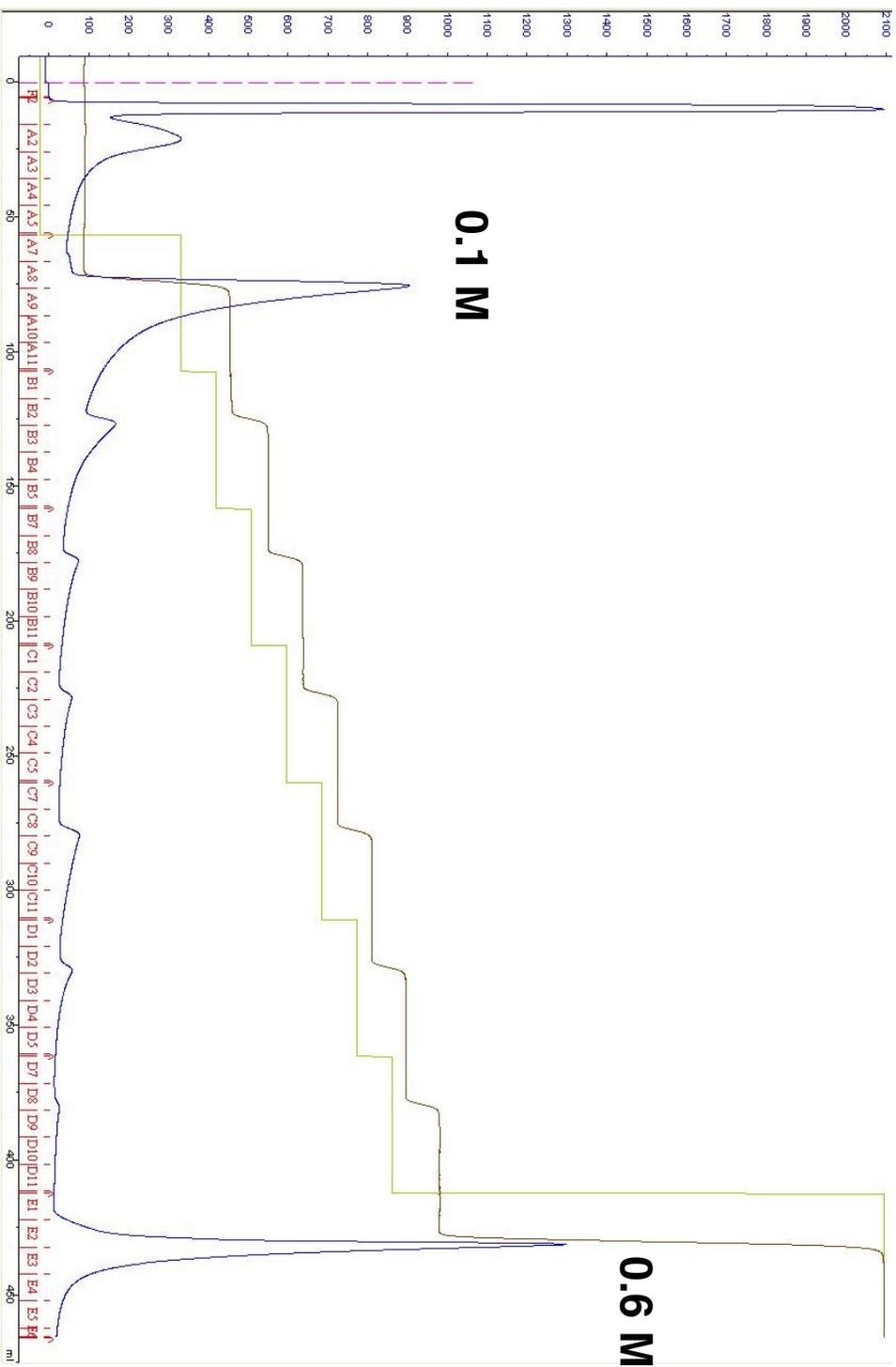
Figure 10 | The Mono Q chromatogram with a load volume of 4.5 mL. Each step is 2.5 column volumes (20 mL=1CV), for 9 steps total at a flow of 3 mL/minute. The steps were 0, 10, 12.5, 15, 17.5, 20, 22.5, 25, and 60% Buffer B. Buffer A: 50 mM Tris 1mM DTT pH 7.4, Buffer B: 50 mM Tris 1mM DTT 1M NaCl pH 7.4 at a flow rate of 3 mL per minute. Each eluted fraction was 10 mL.
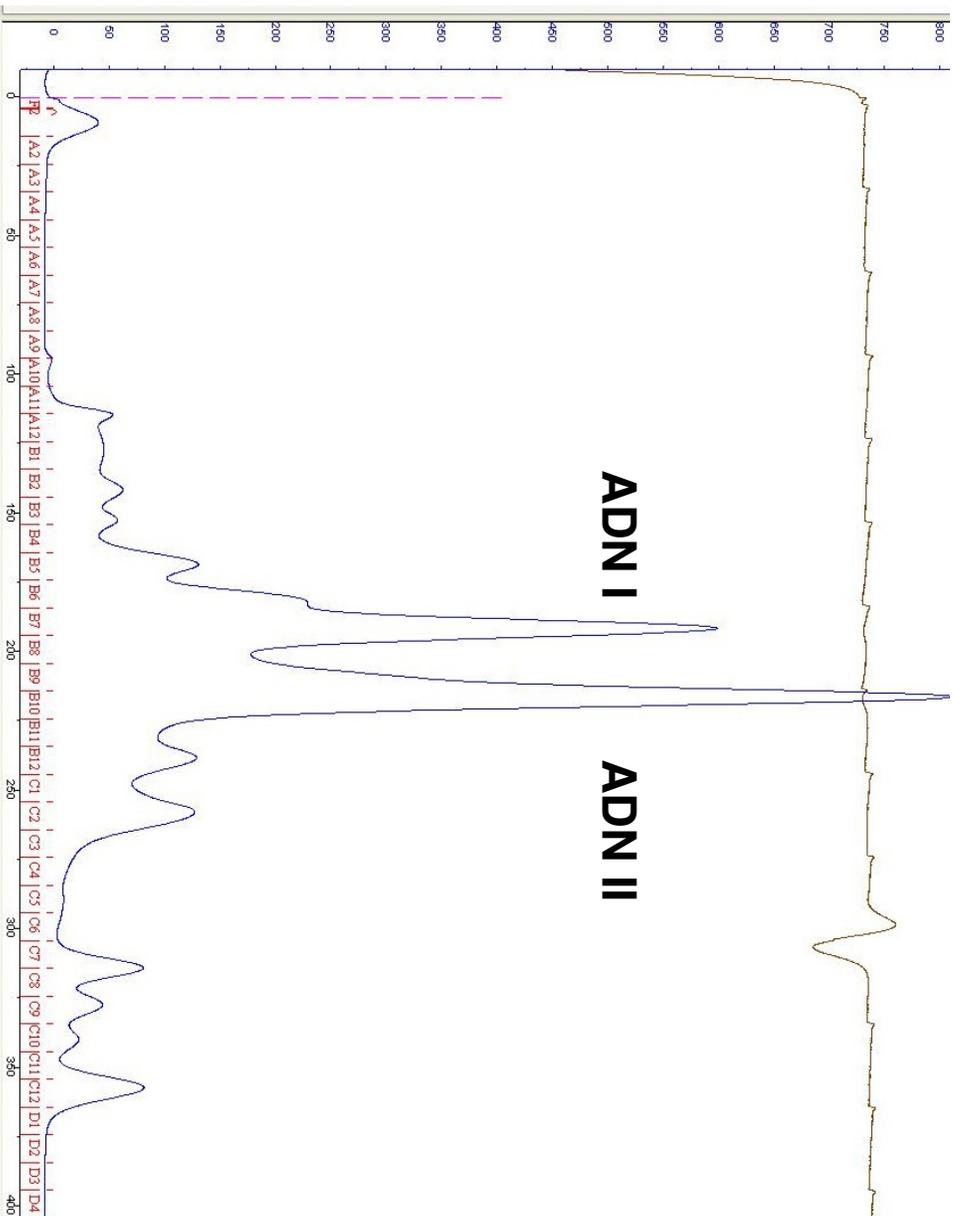
Figure 11 | Superdex S200 size exclusion chromatogram column was equilibrated with 100 mM Tris 300 mM NaCl pH 7.2 for one column volume. The flow was set at 0.5 mL per minute to maximize separation. The 4 mL sample was eluted off the column with 1.5 column volumes with 10 mL per fraction. The prominent peaks I and II were labeled ADN I and ADN II. These fractions were analyzed through SDS-PAGE and adenosine activity on HPLC.

nucleosides I and II (ADN I and ADN II). Both of the pooled fractions demonstrated enzymatic activity. The fraction containing ADN II resulted in one band on SDS- PAGE gel at 25 kDa (Figure 14) and ADN I fraction resulted in a prominent band at 100 kDa with 3-4 faint bands at lower molecular weights. ADN II was pooled and concentrated to
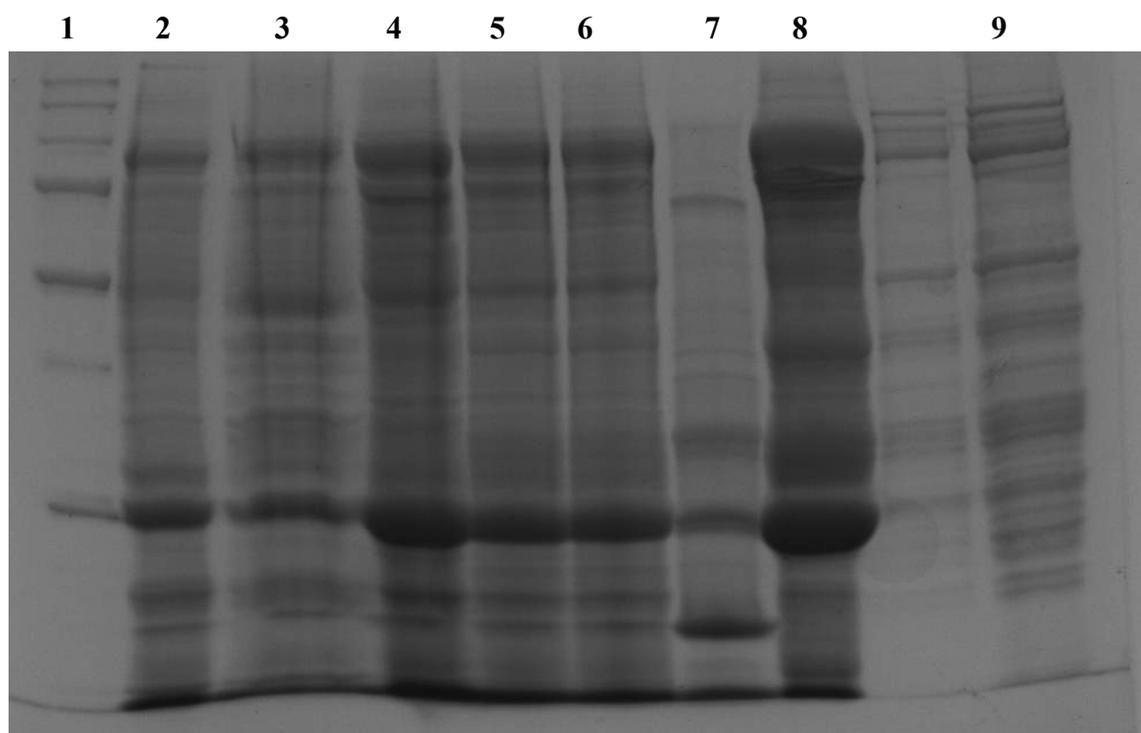
Figure 12 | Mono Q SDS-PAGE Ten μL sample from each purification step was loaded onto 4-12% Tris Glycine SDS PAGE. The samples were loaded as follows: 1: Precision unstained ladder 2: clarified lysate 3: 35% supernatant 4: 70% pellet 5: Dialysis 6: Mono Q load 7: 0.0 M 8: 0.1 M 9. 0.6 M
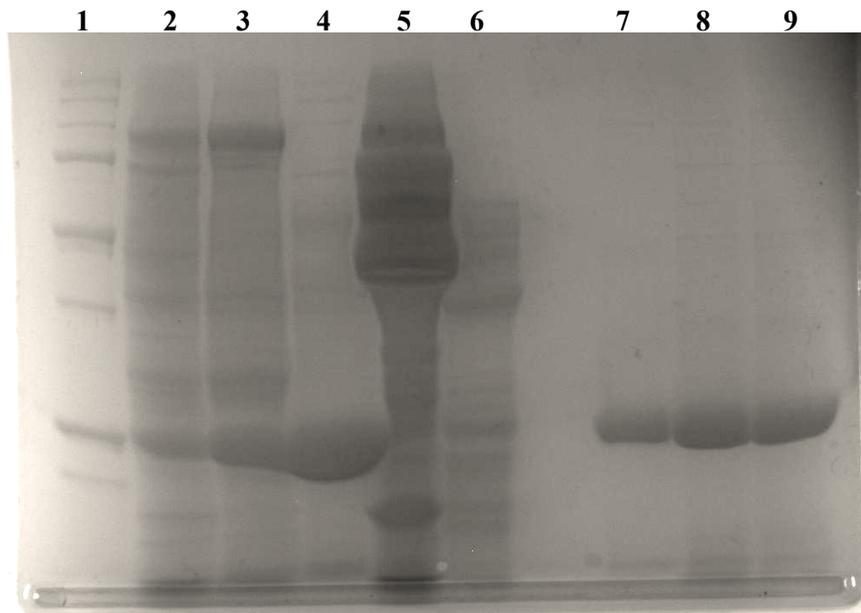
Figure 13 | Size exclusion SDS-PAGE The 25 kDa band was labeled ADN II. The purity of ADN II was compared against other repeat purification attempts. 10 μL samples were loaded as follows: 1. Precision unstained ladder 2. Mono Q load 3. 0.1 M (Mono Q) 4. ADN II 5. 0.6 M (Q) 6. *overflow from lane 5* 7. *empty* 8. 4/20 product 9. 5/1 product 10. 6/1 product. The final purification products from selected dates listed 7-9.

Figure 14 | SDS-PAGE of ADN I and ADN II The purity of the pooled fractions for ADN I and ADN II were analyzed after size exclusion chromatography. A 10 μL sample of each fraction was loaded onto the 4-12% gradient Tris-HCl gel as followed: 1. ADN II 2. ADN I

undergo characterization. ADN I was frozen at -80°C. The purification table in Table 2

revealed a final percent recovery of 2.8 with a specific activity of 0.1845 μmol/hr * mg.

This purification was repeated three times and resulted in ADN II at the same molecular

weight with similar purity and enzymatic activity (Figure 13). The final purification fold

was 103 with a percent recovery of 2.8%. The percent recovery between the 70% pellet

and the Mono Q step were excluded as the purification yield decreased dramatically. This

is evident as the total activity of the two fractions decreased while the final step's activity

increased. The specific activity for each step increased and the purification fold increased

as well. The final specific activity and percent recovery was representative of previous

purification attempts, thus this strategy was reproducible.

Table 2 | **Protein purification table** Each purification step was analyzed for the protein
concentration and enzymatic activity. The specific activity of ADA II was analyzed for
the disappearance of adenosine. The total percent recovery was 2.8.

Step	Volume (mL)	Total Protein (mg)	Total Activity (μmol/hr)	Specific Activity (μmol/hr *mg)	Purification Fold	% Recovery
Clarified Lysate	315	5179.7	93.809	0.0018	1	100
35 % supernatant	340	633.7	7.64	0.0120	6.7	8.1
70% pellet	20	349.5	0.906	0.025	14	—
Mono Q	5	21.21	0.583	0.027	15	—
Size Exclusion	4	14.14	2.608	0.1845	103	2.8

Determination of adenosine enzymatic activity using HPLC

The enzymatic activity of every step in the purification process was checked using a reverse-phase C18 HPLC column. A reaction mixture of 1 mM adenosine in 50 mM Tris pH 7.5 buffer was created using a volumetric flask and 1 mL aliquots were transferred to an HPLC sample vial. One hundred μL of the sample protein was added to the vial for analysis in 98% 10 mM ammonium phosphate pH 5.2 and 2% methanol. The enzymatic activity was observed by the measured rate of disappearance, or decrease in area, of adenosine as it was converted to products. This rate was adjusted by multiplying the volume of protein added and the total volume of the sample to yield the total activity of the sample. This method of analysis was selected rather than the ammonia production assay (34) because ANA II exhibited both nucleosidase and deaminase activity. In Figures 15,16,17,18, an HPLC chromatogram of the beginning, middle, and end of the reaction was analyzed for the reaction products.

In the beginning of the reaction (Figure 15), an unidentified peak with a retention time of 2.03 minutes appeared. As the reaction continued, this peak slowly disappeared as both adenine and inosine were formed. It can be noted that adenine and inosine would often co-elute (Figure 15). As the reaction neared completion adenine and inosine were decreasing as hypoxanthine continued to be generated. In order to generate hypoxanthine, adenosine could be deaminated to inosine and then hydrolyzed to hypoxanthine by a nucleosidase. It is also plausible for a nucleosidase to hydrolyze adenosine to adenine, and then adenine be deaminated to generate hypoxanthine. Hypoxanthine was generated
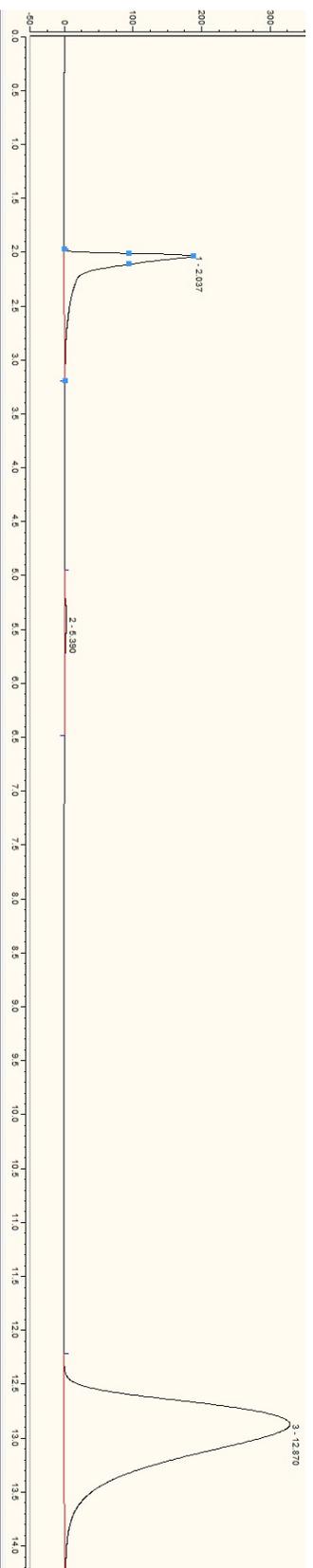
Figure 15 | Reaction mixture 4 hours after addition of enzyme An unidentified peak first appears at 2 minutes with a peak area of 26.22238 mAU *min. Inosine and adenine were beginning to be formed appearing at 5.3 minutes with a peak area of 1.6191 mAU*min. Adenosine remained with a peak area of 193.6177 mAu*min appearing at the mention time 13,5 minutes.
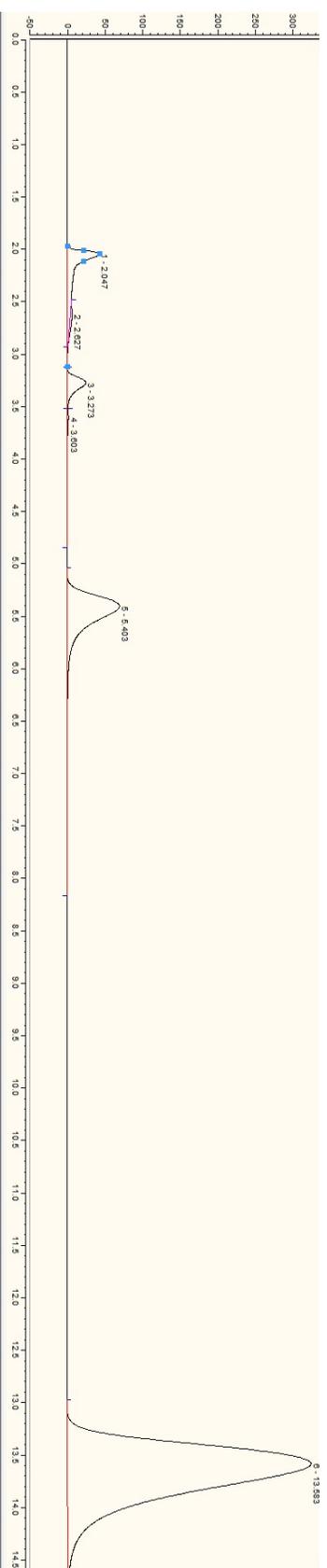
Figure 16 | Reaction mixture 10 hours after addition of enzyme The concentration of inosine/adenine increased (22.6498 mAU*min,). Hypoxanthine was beginning to be formed (3.8523 mAU* min evident by its appearance at 3.2 minutes. Adenosine decreased to 166.49 mAU*min,.
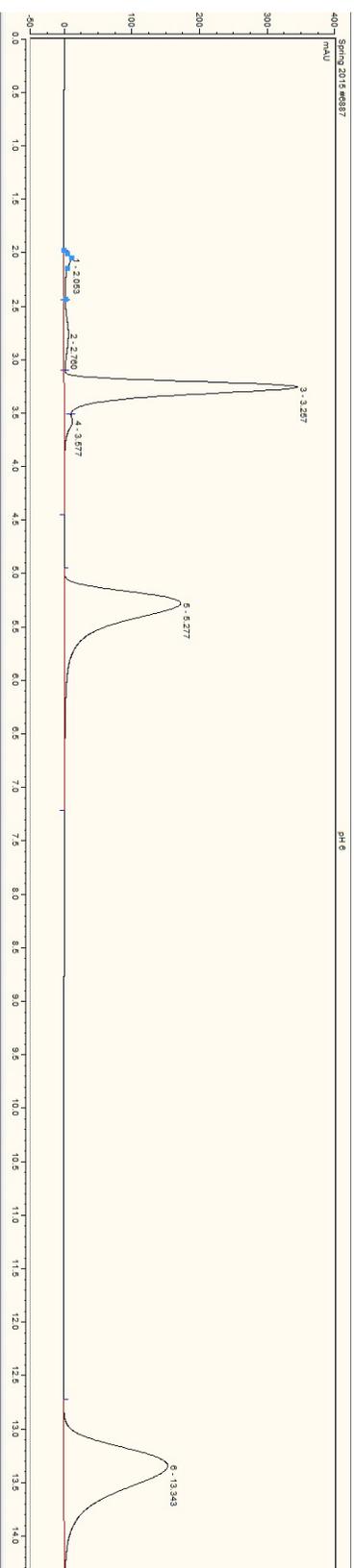
Figure 17 | Reaction mixture 20 hours after addition of enzyme Hypoxanthine was still increasing (50 mAU *min), while adenosine decreased (74.98 mAU*min,) . Yet, the inosine/adenine peak increased as well (58 mAU *min).
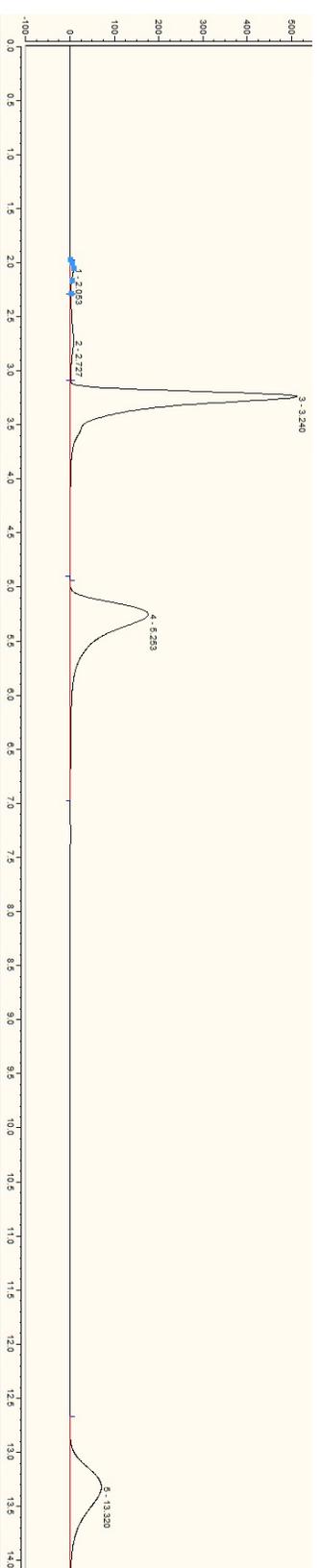
Figure 18 | Reaction mixture 28 hours after addition of enzyme Hypoxanthine peak area increased (83.4 mAu *min,) . The inosine/adenine peak decreased (59.6 mAu*min,), and adenosine peak was nearly gone (35.2 mAu*min,)

as inosine and adenine formed thus suggesting that ADN II was a bi functional enzyme. Figure 18 shows the final stages of the reaction as adenosine was depleted with adenine and inosine solely contributing to the formation of the final reaction product, hypoxanthine. The reaction products were confirmed using Sigma Aldrich nucleoside standards. The retention times of each product at a 1 mM concentration are shown in Table 3.

Table 3 | The retention time of various nucleoside standards were analyzed on a reverse phase HPLC column with the mobile phase 98% 10 mM ammonium phosphate pH 5.2 buffer and 2% HPLC grade methanol. The 1 mM standards were dissolved in pH 6 Teorell-Stenhagen buffer.

Standard (1 mM)	Retention Time (minutes)
Hypoxanthine	3.2
Adenine	5.3
Inosine	5.2
Adenosine	13.3

Determination of native molecular weight

It had been previously determined that the subunit molecular weight of ADN II was 26 kDa (35). The native molecular weight of ADN II was determined by comparing it to the known molecular weights of protein standards in size exclusion chromatography. A protein standard was generated using Blue Dextran (2,000 kDa), carbonic anyhdrase (29 kDa), beta amylase (200 kDa), alcohol dehydrogenase (150 kDa), and cytochrome C

(12 kDa) in 50 mM Tris pH 7.2. The standard was applied to the Superdex 26/60 S200

size exclusion column at a flow rate of 0.5 mL per minute. These experimental conditions

were selected to ensure the protein standards retention times were determined under the

same conditions used to elute the purified proteins, ADN I and ADN II. A linear

regression analysis (Figure 19) of the standards revealed the molecular weights of ADN I

and II were 113 kDa and   67 kDa respectively. Combining data from size exclusion

chromatography and SDS-PAGE , ADN I exists as a a dimer, while ADN II exists as a

dimer or trimer. In order to confirm the purity of the final sample, 1 mL of ADN I was re-

applied to the Superdex   26/60 S200 column and 1 mL of ADN II was applied to

Superdex 26/60 S100 column. The subsequent chromatograms are shown in (Figures 20

and 21).

Elution profile of protein standards in Superdex 26/60 S200

$y = -0.009x + 6.7812$

$R^2 = 0.99213$
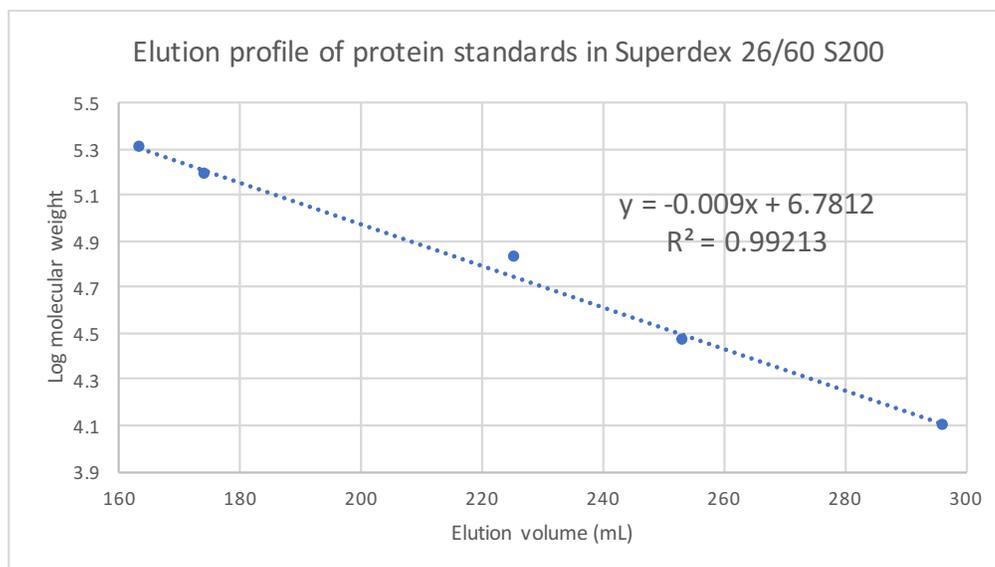
Figure 19 | Linear regression analysis of protein standard molecular weight elution profile The experimental parameters were the same for the size exclusion step within the protein purification (100 mM Tris 300 mM NaCl pH 7.2, flow rate 0.5 mL/min) .
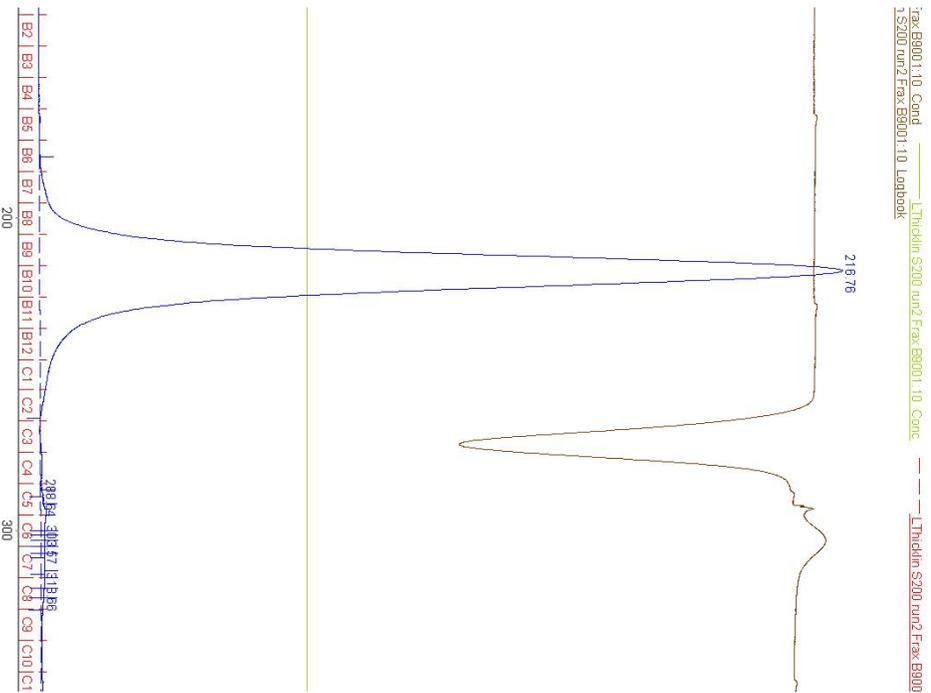
Figure 20 | Size exclusion of ADN I One mL of ADN I was loaded on Superdex 26/60 S200 column. ADN I eluted in 100 mM Tris 300 mM NaCl pH 7.2 at a flow rate of 1 mL per minute.
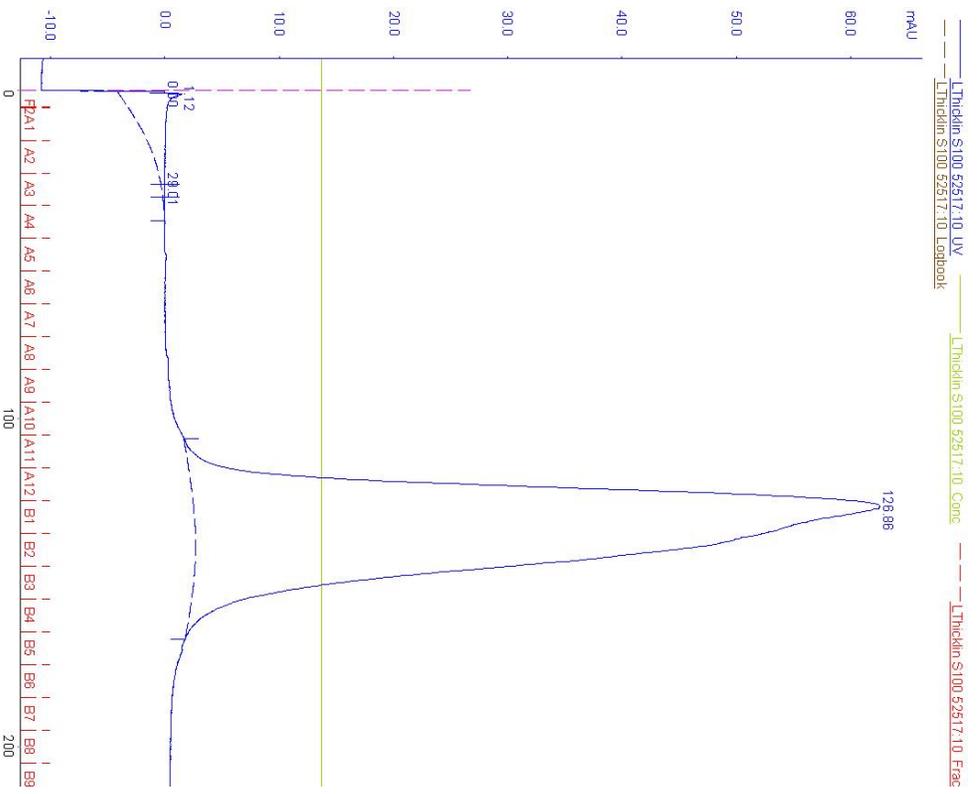
Figure 21 | Size exclusion of ADN II One mL of ADN II was loaded on Superdex 26/60 S100 column. ADN II eluted in 100 mM Tris 300 mM NaCl pH 7.2 at a flow rate of 1 mL per minute.

displayed only a single peak corresponding to the purified protein. The enzymatic activity and purity were retained after chromatography.

The native molecular weights of ADN I and ADNII were determined to be 113 kDa and 67 kDa. ADN II molecular weight was consistent with the native molecular weight of various nucleosidases such as *Azotobacter vinelandii* at 70 kDa (17), Barley leaf extracts at 60 kDa (38), and Coffee arabica young leaves at 72 kDa (39). ADN I molecular weight was very large, yet still plausible as the *Crithidia* nucleosidase molecular weight was 143 kDa.

Determination of optimum pH

The optimum pH for enzymatic activity was determined by analyzing the conversion rate of 1 mM adenosine and 1 mM inosine to products. The substrates were in Teorell-Stenhagen universal buffer (36*)*. This buffer was selected as it contained two components that can produce buffering capabilities across a broad pH range. Moreover pH dependent enzymatic activity analysis using different buffer systems can alter results. "This is [however] an unsatisfactory procedure, due to the varying activities of the enzyme in different buffers. [Moreover] Components of buffers may have stabilizing or destabilizing influence on protein structure and activity (36)." Figures 22 and 23 displayed a bell-shaped enzymatic activity vs. pH curve for adenosine and inosine respetively. The optimum pH for adenosine deaminase/nucleosidase activity was slightly above 6 and the optimum pH for inosine nucleosidase activity was slightly below 6.
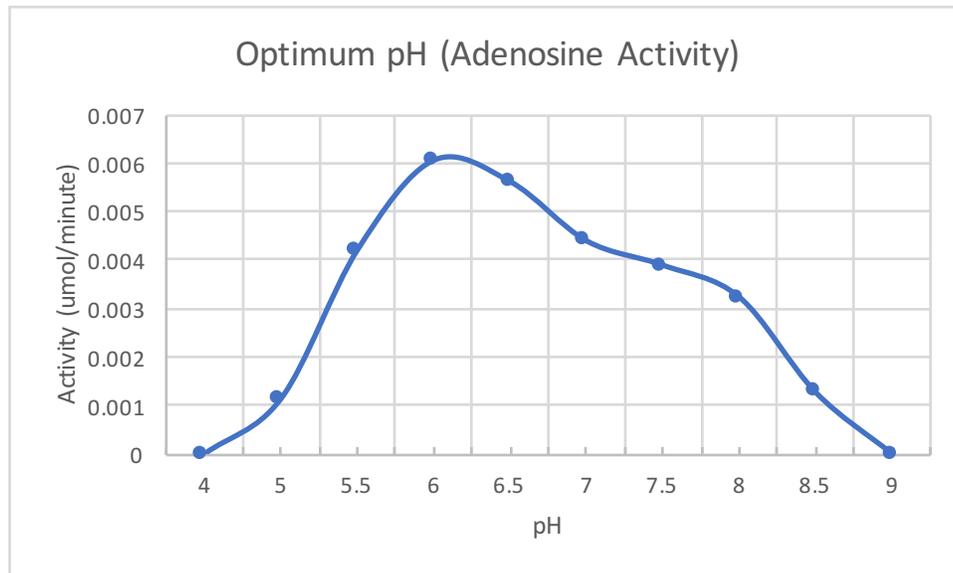
Figure 22 | Optimum pH of adenosine activity was analyzed by a 1 mL reaction mixture of 1 mM adenosine in varying pH of Teorell-Stenhagen buffer with 0.5 μg/μL of enzyme added. The optimum pH was determined to be between 6 and 6.5.
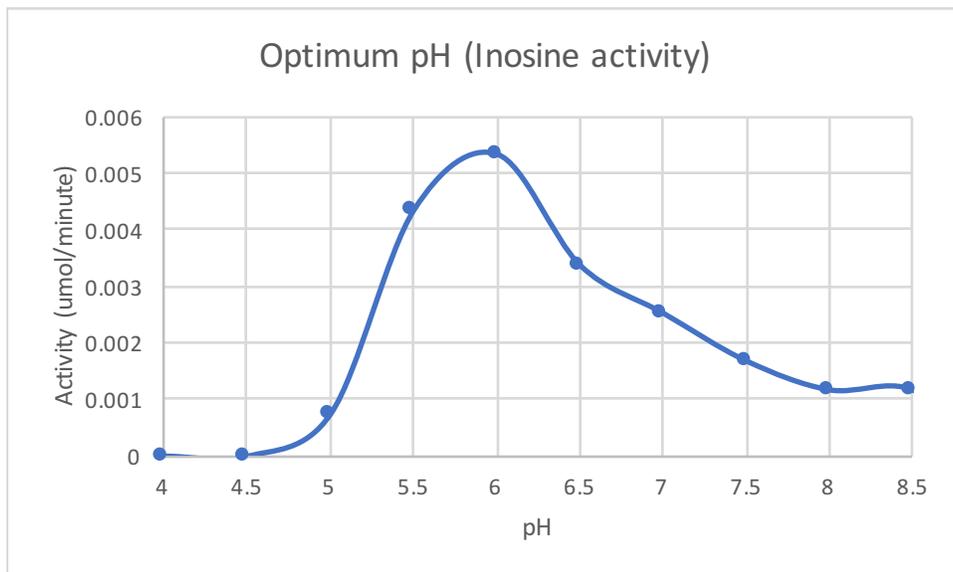
Figure 23 | Optimum pH of inosine activity was analyzed by a 1 mL reaction mixture of 1 mM inosine in varying pH of Teorell-Stenhagen buffer with 0.5 μg/μL of enzyme added. The optimum pH was determined to be 6.

For inosine, 82 % of the activity was retained at pH 5.5, and 22 % of the activity was retained at pH 5. However at pH 6.5 63 % of the activity remained and continued to decrease as 47 % activity remained at pH 7. For adenosine, 93% of the activity was retained at pH 6.5. Sixty-four percent of the activity was retained at physiological pH, 7.5. Yet, 69 % of the activity was retained at pH 5.5.

The proposed active site and catalytic mechanism for adenosine deaminase and inosine nucleosidase are highly similar in amino acid residues. The amino acids shared amongst the two active sites are aspartic acid and glutamic acid.

Within the inosine nucleosidase active site, protonation of N7 of the inosine imidazole ring further activates the leaving group to promote the cleavage of bond between ribose and inosine base. Conversely, the protonated state of the imidazole side chain of histidine within the adenosine deaminase active site is essential for the coordination and the stabilization of the hydroxide nucleophile to attack carbon 6 of inosine (9). Histidine has a side chain pKa of approximately 6 (40). Thus an optimum pH below the pKa ensures histidine is in a protonated state and thus supports the notion of deaminase activity.

Furthermore, a recent study of the variability of histidine side chain pKa values differed from the expected pKa 6 nature of the residue. "It has been found that buried environments of histidines do not always result in acidic pKas. Instead, the variability of histidine pKas increase for residues where the majority of the side chain is buried (41)."

The preferred acidic solvent environment and the protonation state of histidine could provide insight to the true deaminase and nucleosidase mechanism for the purified enzyme.

Determination of oligomerization state

A 12% Native-PAGE was utilized to visualize and separate the oligomers based on charge and pH difference. In order to separate the oligomers, the protein sample was heated at 75 °C for varying times. Fifty μL of enzyme in 50 μL of Teorell-Stenhagen pH 6 universal buffer was heated 0 (control) 5, 10, 30, 60, and 90 minutes. Figure 24 shows ADN II separating into 3 bands after heating for 5 minutes. Two of the bands appear to be shifted and separated from each other, whereas the third band was near the separating line
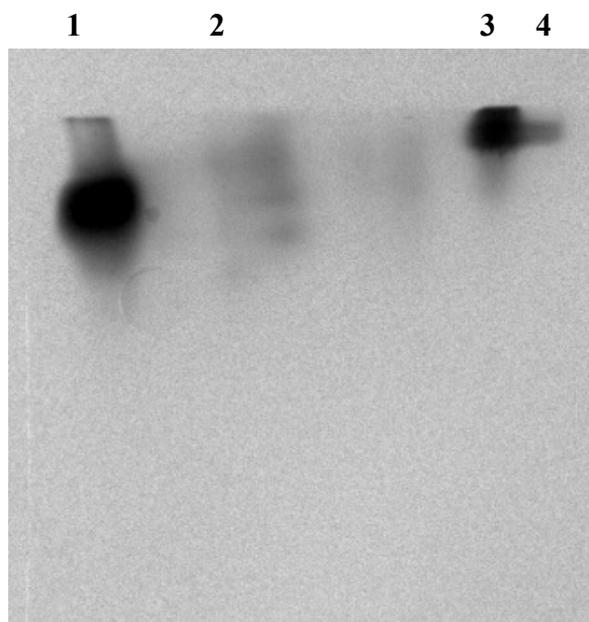
Figure 24 | Native PAGE analysis of various reaction samples of heated ADN I and ADN II. The enzyme precipitated out of solution at high temperature causing very little protein to be loaded on the gel. Thus the wells appear empty. The samples were loaded as followed: 1. ADN II control 2. ADN II 5 minutes 3. ADN II control 4. ADN II heat 5 minutes

of the stacking and resolving gel was deemed inconclusive. ADN I was heated for 5minutes and separated into 2 bands that resolved close together. A prominent issue with heating the reaction was the solubility of the enzyme. As the enzyme was heated, the enzyme precipitated out of solution. It was determined that heating ADN II beyond five minutes resulted in protein aggregation.

Michaelis-Menten kinetic analysis of inosine

The Michaelis-Menten constant for inosine was tested for ADN II. The inosine concentration was varied using the concentrations 25, 50, 100, 250, 500, 750, and 1000 μM. The velocity of the enzymatic reaction was calculated using the standard HPLC enzymatic activity assay procedures. The Km was determined to be 268 μM ± 78 μM with a Vmax of 0.0112 ± 0.005 umol/hour. Figure 25 displays the Michaelis-Menten plot of the data as well as a Lineweaver-Burk plot in Figure 26. In order to calculate a more reliable binding constant, the linear regression from the Lineweaver-Burk plot was utilized (33). The experiment was repeated twice and the Km was calculated independently and averaged together. The Km for inosine was slightly higher compared to the inosine Km values from other plants such as the Jerusalem artichoke shoot, which had a Km for inosine at 2.5 uM (19). Yet *Azobacter vinelandii* exhibited a inosine Km value for 650 μM at pH 9 (17). The higher pH preference of the protozoa asserts the active site may between the two must different from as ADN II exhibits both deaminase and nucleosidase enzymatic activity. ADN II was able to metabolize different nucleosides
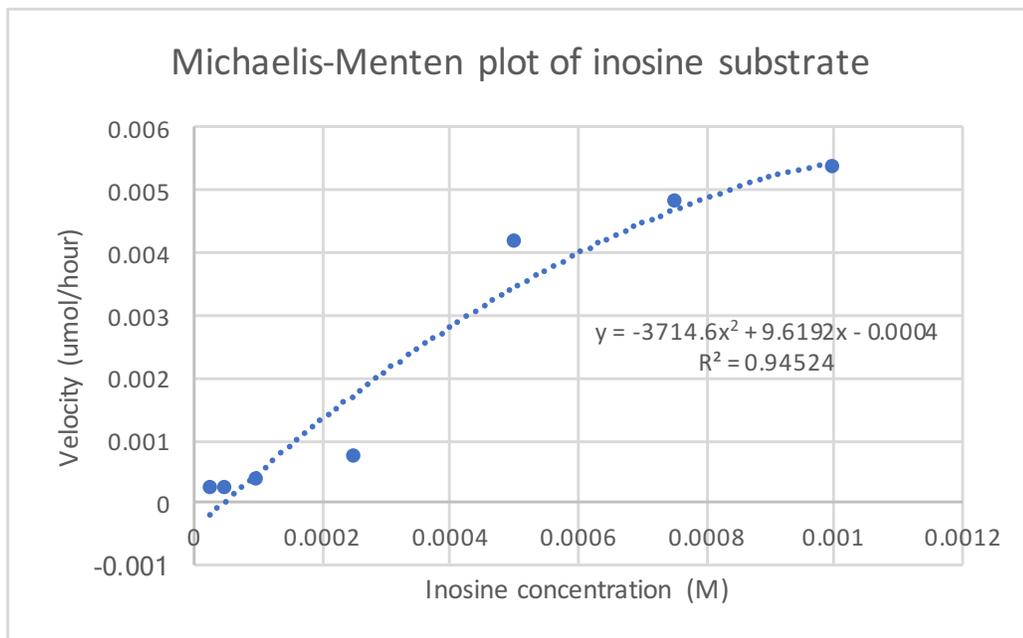
Figure 25 | **Michaelis-Menten plot of inosine** was generated by plotting the reaction velocity versus the inosine substrate concentration. A non-linear regression was performed yet the analyzed value of Km and Vmax was determined from the Lineweaver-Burk plot.
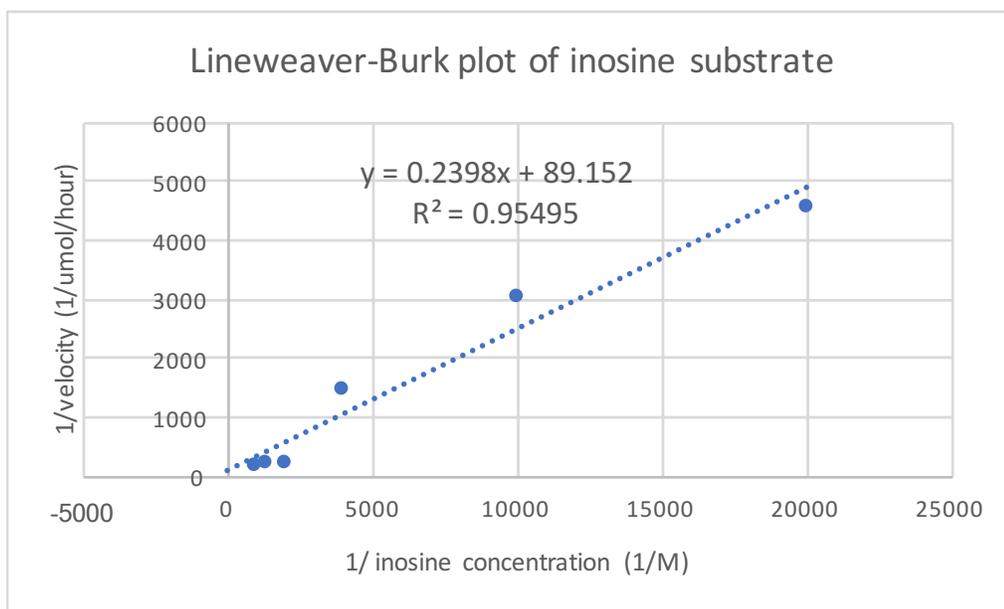
Figure 26 | **Lineweaver-Burk plot of inosine** was generated by plotting the inverse of reaction velocity versus inverse inosine substrate concentration. A linear regression of the data a binding constant of inosine to be 268 μM ± 78 μM

such as uridine, cytidine, and thymine (35), thus it is relatively non-specific in substrate

binding. Furthermore, a higher specificity in substrate binding for inosine would result in

a lower Km.

CHAPTER IV

CONCLUSIONS

Nucleotides are essential biomolecules due to their imperative role in energy transfer, metabolism, intercellular signaling, and much more (1). Plants such as the Alaska pea rely on the purine salvage pathway to recycle bases to maintain pools of nucleotides. Nucleoside hydrolases and deaminases are essential in the purine salvage pathway Deaminases catalyze the hydrolysis of an amine to a carbonyl. Nucleosidases catalyze the hydrolysis of the N-glycosidic bond in purines to generate ribose and purine base.

A packet of Arejas wilt resistant Alaska pea twenty grams seeds were sterilized and germinated for four days. Multiple strategies using different ion exchange chromatography columns were adopted to improve the purity while minimizing target protein loss. Current literature purification of nucelosidases and deaminases (23, 24) utilized a DEAE ion exchange column with a step wise NaCl gradient. However, this technique was largely unsuccessful as there were multiple eluted impure peak fractions with enzymatic activity.

In order to generate a more selective purification the following changes were adopted: utilizing a Mono Q ion exchange column (a stronger anion exchanger), the buffer was switched from potassium phosphate to Tris-Base (more thermally stable), 1 mM DTT was added when dialyzing and eluting from column, and the buffer pH was

shifted from 7 to a more basic 7.5. The changes to the ion exchange chromatography step resulted in greater resolution and purity of the target protein from the sample. Size exclusion chromatography was utilized to resolve the two molecular weight proteins. The 100 kDa protein was labeled ADN I, or adenosine deaminating nucleosidase I, and the 67 kDa protein as ADN II, adenosine deaminating nucleosidase II.

The enzymatic activity of ANA II was analyzed using HPLC reverse phase chromatography. The enzymatic activity was observed by the measured rate of disappearance, or decrease in area, of adenosine as it was converted to products. It was determined from the products produced that the purified protein was a bifunctional enzyme. Thus it was referred to as a deaminating nucleosidase.

The native molecular weight of the purified protein was determined using a Superdex 200 size exclusion column. A linear regression analysis of the standards revealed the molecular weights of ADN I and II were 113 kDa and 67 kDa respectively. Combining data from size exclusion chromatography and SDS-PAGE , ADN I exists as a a dimer, while ADN II exists as a dimer or trimer.

A Native-PAGE was performed to further elucidate the oligomerization of ADN II. The samples were heated to induce thermal unfolding of the protein. ADN II separated into 2 shifted bands and 1 faint band after heating for 5 minutes. ADN I separated into 2 bands that resolved close together. This further confirmed ADN II as either a dimer or trimer and ADN I as a dimer.

The optimum pH for enzymatic activity was determined by analyzing the conversion rate of 1 mM adenosine and 1 mM inosine to products. The optimum pH for adenosine deaminase/nucleosidase activity was slightly above 6 and the optimum pH for inosine nucleosidase activity was 6. The Michaelis-Menten constant for inosine was tested for ADN II. The Km, for inosine was tested at the optimum pH and was determined to be 268 μM ± 78 μM with a Vmax of 0.0112 ± 0.005 μmol/hour.

REFERENCES

1. Voet, D.; Voet, J.; Pratt, C. *Fundamentals of Biochemistry*; Wiley, **2008** Ed.3; p 39.

2. Voet, D.; Voet, J.; Pratt, C. *Fundamentals of Biochemistry*; Wiley, **2008** Ed.3; p 40-42.

3. DNA-structure. http://www.chemguide.co.uk/organicprops/aminoacids/dna1.html (accessed November 2016).

4. Metabolism of Glycine (Part 2)- Metabolic role and clinical significance http://www.namrata.co/metabolism-of-glycine-part-2-metabolic-role-and-clinical-significance/ (accessed November 2016).

5. Voet, D.; Voet, J.; Pratt, C. *Fundamentals of Biochemistry*; Wiley, **2008** Ed.3; p 818-819.

6. Henikoff, S. Multifunctional polypeptides for purine *de novo* synthesis. *Bioessay*s, **2008,** 6, p 8–13. doi:10.1002/bies.950060104.

7. Stoyanov A., Petrova P., Lyutskanova D., Lahtchev K., Structural and functional analysis of PUR2, 5 gene encoding bifunctional enzyme of *de novo* purine biosynthesis in *Ogataea* (Hansenula) polymorpha CBS 4732T. *Microbiological Research,* **2014,** 169, p 378-387.

8. 1VFL: Adenosine deaminase http://www.rcsb.org/pdb/explore.do?structureId=1VFL (accessed November 2016).

9. Cristalli G., Costanzi S., Lambertucci C., Lupidi G., Vittori S., Volpini R., Campioni E., Adenosine deaminase: Functional implications and different classes of inhibitors. *Medicinal Research Reviews* **2001** 21, p 105-128.

10. Kinoshita T., Nishio N., Sato A., Murata M., Crystallization and preliminary analysis of bovine adenosine deaminase *Acta Cryst* **1999** 27, p 1-5.

11. O'Hara F., The Baran laboratory http://www.scripps.edu/baran/images/grpmtgpdf/OHara_Jun_12.pdf (accessed November 2016).

12. Kurtz, J.; Exinge, F.; Erbs, F.; Jund, R The URH1 Uridine Ribohydrolase of Saccharomyces Cerevisiae. *Current Genetics* **2002**, 41, p 132-141.

13. Pellé, R.; Schramm, V. L.; Parkin, D. W. Molecular Cloning and Expression of a Purine-specific N-ribohydrolase from Trypanosoma Brucei Brucei. Sequence, Expression, and Molecular Analysis. *The Journal of Biological Chemistry* **1998**, 273, p 2118-2126.

14. Cui, L.; Rajasekariah, G.; Martin, S. K. A Nonspecific Nucleoside Hydrolase from Leishmania Donovani: Implications for Purine Salvage by the Parasite. *Gene* **2001,** 280, p 1530-162.

15. Versees, W., Steyaert, J. Catalysis by Nucleoside Hydrolases. *Current Opinion in Structural Biology* **2003**, 13, p 731-738.

16. Garret E., Mehta PJ., Solvolysis of adenine nucleosides. I. Effects of sugars and adenine substituents on acid solvolyses *Journal of the American Chemical Society* **1972,** 94, p 8532-8541.

17. Yoshino M., Tsukada T., Tsushima K., Inosine nucleosidase from *Azotobacter vinelandii* purification and properties *Archives of Microbiology* **1978** 119, p 549-564.

18. Guranowksi A. Purine Catabolism in Plants *Plant Physiology* **1982,** 70, p 34-349.

19. Le Floc'h F., Lafleuriel J., The purine nucleosidase from Jerusalem artichoke shoots *Phytochemistry* **1981,** 20, p 2127-2129.

20. Parkin D.,Horensteingn B.,Abdulahg D., Estupiiang B.,Schrammg V., Nucleoside Hydrolase from *Crithidia fasciculuta Journal of Biological Chemistry 1991,* 266, p 20658-20665.

21. Brawerman G., Chargaff E., Deoxyribonuclease from germinating barley *Journal of Biological Chemistry* **1954,** 210, p 445-454.

22. Ali E.M.M, *Fasciola gigantica*: Purification and characterization of adenosine deaminase *Experimental Parasitology* **2008,** 119, p 285-290.

23. Banerjee R., Banerjee S., Sarkar P., Pradhan NK., Isolation, purification and characterization of *Plasmodium yoelii* adenosine deaminase for clinical use *Journal of Advanced Pharmacy Education & Research* **2014,** 4, p 216-220.

24. Seed germination and dormancy http://www.biologyreference.com/Re-Se/Seed-Germination-and-Dormancy.html *(accessed November 2016).*

25. Laing W., Christeller J., Extraction of proteins from plant tissues *Current Protocols in Protein Science* Wiley, **2004**, 4.7.1, 4.7.7.

26. Scopes R., Salting out: Ammonium sulfate precipitation *LabFax* Bios Scientific publishers, Academic Press, **1996**, p 31-32.

27. Good's Buffers http://www.sigmaaldrich.com/life-science/biochemicals/biochemical-products.html?TablePage=14572938 (accessed May 2017).

28. Bradford M.M, A rapid and sensitive method for the quantification of microgram quantities of protein using the principals of protein-dye binding *Analytical Biochemistry* **1976,** 72, p 248-254.

29. Whittaker J.R., Determination of molecular weights of proteins by gel filtration of Sephadex *Analytical Chemistry 1963,* 35, p 1950-1953.

30. Garfin D., Gel electrophoresis of proteins *Essential Cell Biology: Cell structure, A practical approach* Oxford University Press **2003**, 1, p 197-268.

31. Arakawa T., Philo J., Kita Y., Kinetic and thermodynamic analysis of thermal unfolding of recombinant erythopoietin *Bioscience Biotechnology Biochemistry* **2001,** 65, p 1321-1327.

32. Teorell T., Stenhagen E., Electrophoretic properties of thymonucleic acid, *Transactions of the Faraday Society* **1939,** 35, p 743-750.

33. Engel P.C., Enzyme Kinetics *LabFax* Bios Scientific Publishing, Academic press **1996,** p 77-112.

34. Giusti, G., Adenosine deaminase. In: Bergmeyer, H.U. (Ed.), *Methods of Enzymatic Analysis*. Academic Press, New York, **1974,** p 1092–1099.

35. Shamsuddin A., Characterization of Adenosine nucleosidase from Alaska Pea *ProQuest* **2014.**

36. Bisswanger H., Enzyme Assays *Perspectives in Science* **2014,** 1, p 41-55.

37. Alshaiban S., Study of nucleoside degreading enzyme activities in bean, organic bean, okra, organic okra, squash, and organic squash *ProQuest* **2015.**

38. Guranowski A., Schneider Z., Purification and characterization of adenosine nucleosidase from barley leaves. *Biochemical et Biophysica Acta (BBA)-Enzymology* **1977,** 482, p 145-158.

39. Campos A., Rijo-Johansen M., Carneiro M., Fevereiro P., Purification and characterization of adenosine nucleosides from *Coffee arabica* young leaves. *Phytochemistry* **2005,** 66, p 147-151.

40. Voet, D.; Voet, J.; Pratt, C. *Fundamentals of Biochemistry*; Wiley, **2008** 3, p 76-77.

41. Edgcomb S., Murphy K., Variability in the pKa of Histidine side-chain correlates with burial within proteins *Proteins: Structure, function, and genetics* **2002,** 49, p 1-6.

42. Marmocchi F., Lupidi G., Venardi G., Riva F., Adenosine deaminase from *Sacchromyces cerevisiae*: purification and characterization. *Biochemistry International* **1987,** 14, p 569-580.

43. Unkyu K., Garner T., Sanford T., Speicher D., Murray J., Nishikura K., Purification and characterization of double-stranded RNA adenosine deaminase from bovine nuclear extracts. *The Journal of Biological Chemistry* **1994,** 269, p 13480-13489.

44. Pymol software systems. https://www.pymol.org.